Metagenome-based analysis of the functional potential of a marine sediment community dominated by ANME-2c

Thesis submitted in partial fulfillment of the requirements for the degree of Master of Science

Autumn 2015
Faculty of Mathematics and Natural Sciences/Department of Biology/ Center for Geobiology (CGB)
BY: SEPIDEH MOSTAFAVI
Supervised by: Dr. Ida Helene Steen/ Dr. Runar Stokke

Acknowledgment

The work described in this thesis was accomplished at the Center for Geobiology (CGB), at the Faculty of Mathematics and Natural Sciences/Department of Biology, University of Bergen, in the period from August 2013 to October 2015.

Now, at the end of this rough period, I take this opportunity to express my very great appreciations and deep regards to my academic supervisor, Dr. Ida Helene Steen, who had the pivotal role in completing this project. A supportive teacher, who guided me in every step of this project and the one, whose useful comments, taught me a lot. Without her serious and kind monitoring and her patient supports, it was impossible to finish the rough course of this thesis.

I would also like to express my sincere gratitude to my co-supervisor, Dr. Runnar Stokke, for providing me a valuable knowledge and is help to complete this task through various stages. A trustworthy person that was open to anytime question and whose valuable suggestions were the great support during the development of this research work.

I wish to thank Dr. Irene Roalkvam for processing the samples and her useful recommendation and valuable assistance in the lab. Furthermore, I would like to thank Dr. Håkon Dahle for his effective advice and various people at CGB center for creating a friendly working environment.

Finally, my warmest thanks go to my parents for believing in me and providing me this opportunity, for their constant, unquestionable encouragements and care during tough times.

Bergen October 2015

Abbreviation

ANME	Anaerobic methanotrophic archaea
AprA	Adenylylsulfate reductase (Apr) subunit A
AprB	Adenylylsulfate reductase (Apr) subunit B
APS	Adenosine 5'-phosphosulfate
AOM	Anaerobic oxidation of methane
bp	Base pairs
cmbsf	Cm below the seafloor
CH_4	Methane
CO	Carbon monoxide
CO_2	Carbon dioxide
CoA	Co-enzyme A
DBB	*Desulfobulbus*
DsrA	Dissimilatory sulfite reductase (Dsr) subunit A
DsrB	Dissimilatory sulfite reductase (Dsr) subunit B
DsrC	Dissimilatory sulfite reductase (Dsr) subunit C
DSS	*Desulfosarcina–Desulfococcus*
H_2S	Hydrogen sulfide
H_4MPT	Tetrahydromethanopetrin
McrA	Methyl CoM reductase (Mcr) subunit A
Mer	Coenzyme F_{420}- dependent N_5N_{10}-methylene tetrahydromethanopterin reductase
MFR	Methanofuran
N_2	Molecular nitrogen
NO_3^-	Nitrate
NO_2^-	Nitrite
PAPS	3′-phosphoadenosine-5′-phosphosulfate
Qmo	quinone-interacting membrane-bound oxidoreductase
RAST	Rapid Annotations using Subsystems Technology
rRNA	Ribosomal RNA
rTCA	Reductive Tricarboxylic acid (TCA) cycle
Sat	Sulfate adenylyltransferase
S^0	Sulfur
SO_4^{2-}	Sulfate
SO_3^{2-}	Sulfite
SRB	Sulfate reducing bacteria
SMTZ	Sulfate-methane transition zone
TCA	Tricarboxylic acid (TCA) cycle- Krebs cycle
THF	Tetra hydro folate

Abstract

Methane is the most abundant hydrocarbon in the atmosphere and after CO_2; it contributes for 14% of global greenhouse gas emissions. Marine sediments are a large reservoir of methane where approximately 80% of the methane is formed through a biological process known as methanogenesis by methanogenic archaea. Despite the high rates of CH_4 production in marine sediments, about 90% of methane flux from sediment is recycled through the microbial process, anaerobic oxidation of methane (AOM) with sulfate. The AOM is catalyzed by uncultivated anaerobic methanotrophic archaea (ANME-1, 2 and 3) which thus have a crucial role regulating the flux of methane from marine environments to the atmosphere. In this study, the functional potential of an ANME2c-dominated sediment horizon at 20-22cm below the seafloor in the G11 pockmark at Nyegga has been investigated using a metagenomic approach. Total DNA was applied to 454-pyrosequencing and 142.8 MB (1001981 sequence reads) sequence information was assembled into 22706 contigs. The assembled contigs were clustered into 4 bins based on multivariate statistics of tetra-nucleotide frequencies combined with the use of interpolated Markov models, using Metawatt binner tool. Three of the metagenomic bins were imported into RAST for annotation. From the bins, genes encoding phylogenetic marker genes, 16S rRNA, Adenylylsulfate reductase (AprAB) and Methyl CoM reductase (Mcr) subunit A (McrA) were extracted. Phylogenetic analysis suggested that metagenomic bin II was of ANME2c and bin I was of *Desulfobacteraceae*. A complete set of genes encoding enzymes involved in reverse methanogenesis including Coenzyme F_{420}- dependent N_5N_{10}-methylene tetrahydromethanopterin reductase (Mer) and Methyl CoM reductase (Mcr) was observed in the ANME2c bin. In the *Desulfobacteraceae* bin, the enzymes involved in three enzymatic reactions of the dissimilatory sulfate reduction pathway, Sulfate adenylyltransferase (Sat), Adenylylsulfate reductase (AprAB) and Dissimilatory sulfite reductase (DsrABC) were identified. Furthermore, the electron transporter proteins, QmoABC (quinone-interacting membrane-bound oxidoreductase) and DsrMJKOP complexes known to donate electron to AprAB and DsrABC, respectively, wer found in this bin. The presence of CO-dehydrogenase/acetyl-CoA synthase (Fd2−red), the key enzyme of acetyl-coenzyme A (CoA) pathway, in the *Desulfobacteraceae* and ANME-2c bins indicated a potential for CO_2 fixation via this pathway in both groups of microorganisms. The obtained data did not reveal any information about substrate spectrum by the *Desulfobacteraceae* as no genes encoding an uptake hydrogenase, formate dehydrogenase and lactate dehydrogenase were identified. The metagenomic analyses did not support the use of other electron acceptors like nitrate of iron/manganese by the ANME2c population. However, the presence of gene fragments of a nitrogen fixation pathway in methanogenic archaea in the metagenomic data indicated a potential for this process in the community. Altogether, this study has fortified the partnership of ANME-2c and sulfate-reducing bacteria from the *Desulfobacteraceae* family, and revealed new information about other possible aspects of syntrophy, in addition to the methane oxidation coupled to sulfate reduction, in the Nyegga sediments.

Table of Contents

1. Introduction

The sea-bed may not seem like a hospitable habitat. Permanent darkness and isolation from photosynthetic pathways, high pressure and nearly freezing temperature (less than 4°C) characterize the sea-bed as a biologically inert environment. Deep-sea research in the nineteen century revealed that beside the vast desert-like plain of deep sea mud, this large habitat consists of a wide range of environments such as hydrothermal vents, ocean crust, cold-seep, trench and seamounts (Jorgensen and Boetius, 2007, Orcutt et al., 2011). Back in 1850s, Edward Forbes claimed the "azoic hypothesis" which states that no life exists below 300 fathoms (Anderson and Rice, 2006). Subsequently in the 1950s, analysis of sediment samples collected from the Philippine Trench at more than 10,000m depth (Zobell and Morita, 1959) , laid Forbes's theory to rest. Samples were gathered on the Danish-Galathea Deep-sea Expedition and they showed the presence of millions of variable bacteria per gram (Jorgensen and Boetius, 2007, Zobell and Morita, 1959).

All life on earth depends on access to the source of energy and carbon. No photosynthesis exists in the deep sea due to inadequate light at depth, therefore in the dark ocean metabolic strategies are based on chemical redox reactions rather than photosynthesis process (Orcutt et al., 2011). Furthermore, organisms in the dark ocean utilize different respiration pathways. These energy-generating reactions are differently coupled, spatially, temporally and functionally (Jorgensen and Boetius, 2007, Orcutt et al., 2011). In the absence of light, energy is obtained when the coupled redox reactions are thermodynamically favorable and yield enough energy for ATP generation. Redox reactions involve the transfer of electron(s) between compounds; therefore, the metabolic reactions in the dark ocean are dependent upon the availability and speciation of electron donors and acceptors (oxidizable and reduceable compounds, respectively). The contribution of each electron donors and acceptors to the overall metabolic activity in any environment is dependent in part on their availability (Dahle et al., 2015). The dominant electron donors in the dark ocean include organic matter, molecular hydrogen, methane, reduced sulfur compounds, reduced iron and manganese, and ammonium. Oxygen, nitrate, nitrite, manganese and iron oxides, oxidized sulfur compounds and carbon dioxide are available electron acceptors in the dark ocean (Orcutt et al., 2011).

1.1. Methane cycling

Marine sediments are the largest reservoir of methane on earth (Knittel and Boetius, 2009, Reeburgh, 2007). At the continental margins large amount of methane are stored in the subsurface sediments as crystalline methane hydrates, dissolved in pore water and as free gas (Kvenvolden, 1993). Methane is one of the cornerstones of the global carbon cycle. In marine sediments, it is generated through abiotic (Sherwood Lollar et al., 2002, Kelley and Früh-Green, 1999) and/or biotic processes (Kvenvolden and Rogers, 2005). Abiotic formation of methane occurs either by the thermal degradation of buried organic matters (Sherwood Lollar et al., 2002) or by the reaction of H_2 and CO_2 during reaction between mafic (i.e. magnesium and iron-rich)

rocks referred as the serpentinization process (Kelley and Früh-Green, 1999). The abiotic formation of methane represents only a small fraction of methane generation compared to the methane formed via biotic processes in marine environments (Thauer et al., 2008). Microbial production of methane from either CO_2 plus H_2 (Reaction 1), or from methylated compounds (formate, methanol, methylamines…), is known as methanogenesis. Only microorganisms from the *Archaea* domain can perform methanogenesis and biologically produce methane. These microorganisms, called methanogens, are strict anaerobes. All methanogens thus typically exist in anaerobic environments where the only available electron acceptor is CO_2 (Kietavainen and Purkamo, 2015).

$$CO_2 + 4H_2 \rightarrow CH_4 + 2H_2O \quad (1)$$

Globally, about 80% of methane is formed by methanogenic archaea (Orcutt et al., 2011). Produced methane diffuses upwardly and can either served as a substrate for aerobic or anaerobic methane oxidation (AOM) or be emitted to the atmosphere (Liu and Whitman, 2008). In marine sediments, the main niche for AOM is a region of sulfate (SO_4^{2-}) and methane (CH_4) interface known as sulfate-methane transition zone (SMTZ) (Iversen and Jorgensen, 1985). Since the production of methane undergoes bellow the sulfate-rich zone, sulfate is the first electron acceptor candidate for AOM. In this process methane serves as an electron donor and is converted to carbon dioxide (CO_2) and reduced products are served as electron donors in the conversion of SO_4^{2-} to hydrogen sulfide (H_2S) and water (Orcutt et al., 2011).

Methane constitutes 14% of global greenhouse gas emissions (Cui et al., 2015). Although the methane concentration in the atmosphere is lower than the CO_2 concentration, it contributes to ~30% of the anthropogenic warming, with the radiative forcing of 0.48 Wm 2 in 2011, due to its capacity to trap heat in the atmosphere about 25 folds more than CO_2 (Cui et al., 2015). Despite high rates of CH_4 production in marine sediments, 80% of methane flux from sediment is recycled through microbial AOM (Knittel and Boetius, 2009). This process keeps the oceanic methane emission less than 2% of total global methane emission. The concentration of the methane differs from millimolar in marine sediments to nanomolar in ocean waters (Reeburgh, 2007) . Thus, microbial methane oxidation plays an important role for sinking the atmospheric methane and keeping the balance of methane emission to the atmosphere. In other words, it has a great impact on global warming (Boetius et al., 2000a, Orcutt et al., 2011).

1.1.1. Methanogenesis

1.1.1.1. Methanogenes

Seven methanogenic archaeal orders have been identified including *Methanopyrales*, *Methanococcales*, *Methanobacteriales*, *Methanocellales*, and *Methanomicrobiales* and *Methanosarcinales* (Costa and Leigh, 2014, Thauer et al., 2008) and *Methanoplasmatales* (Paul et al., 2012). Hydrogen serves as main electron donor for reduction of CO_2, but formate, carbon monoxide (CO), and certain alcohols can provide the electrons for this process in some

methanogens (Madigan et al., 2015). Hence, they can be categorized into two groups depending on the methane generating pathways: chemolithoautotrophic methanogens and chemoorganotrophic methanogens. The chemolithoautotrophic methanogens use CO_2 and H_2 for all cellular purposes, from production of energy to production of their cellular building blocks, whereas chemoorganotrophic methanogens employ various carbon molecules containing methyl group such as acetate, methanol, methylamines, and methylsulfides as substrates (Kietavainen and Purkamo, 2015).

1.1.1.2. Methanogenesis from CO_2 +H_2

The methanogenesis involves series of biochemical reactions ultimately ending up with the formation of methane. Two different coenzymes participate in this process; 1) C_1 carriers that carry C_1 unit along the enzymatic pathway and 2) the redox coenzymes which donate electrons. The first group is respectively composed of Methanofuran, Methanopterin, Coenzyme M (CoM), and F_{430} coenzyme. The coenzyme F_{420} and 7-mercaptoheptanoylthreonine phosphate (Coenzyme B, CoB) donate electrons through methane formation pathway (Liu and Whitman, 2008).

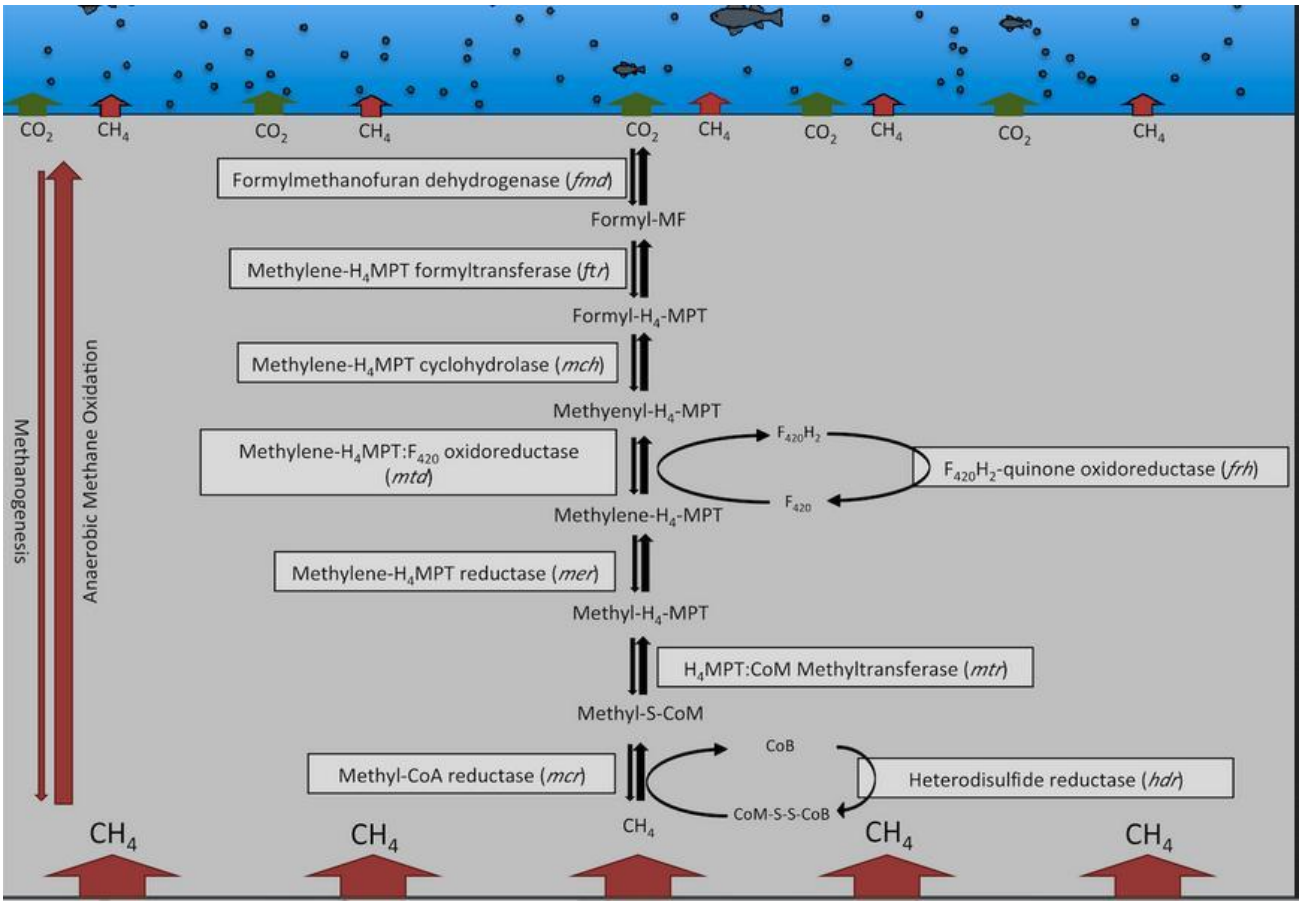

Figure 1. Methanogenesis and AOM through reverse methanogenesis pathway. Adapted from (Hawley et al., 2014).

Methanogenesis (Figure 1.) in which eight electrons are transferred from H_2 to CO_2 is summarized as:

- In the first step, a methanofuran (MFR)-containing enzyme activates CO_2. Methanofuran, through its amino group, binds CO_2 and reduces it to the formyl level. The protein ferredoxin, which is reduced by H_2, is the immediate electron donor.
- The C-1 moiety is transferred to a tetrahydromethanopetrin (H_4MPT)-containing enzyme and forms formyl-H_4MPT. The formyl group is dehydrated to methenyl and subsequently reduced to the methylene and methyl levels forming methyl-H_4MPT. (Two separate steps). Reduced F_{420} supplies electrons for these steps.
- A CoM- containing enzyme accepts the methyl group from methanopterin.
- A methyl reductase (MCR) reduces methyl-CoM to methane. In this reaction coenzyme F_{430} transfers the CH_3 group from CH_3-CoM and forms a Ni^{2+}-CH_3 complex. Then CoB donates electrons to this complex and reduces it to methane forming a disulfide complex of CoM and CoB (CoM-S—S-CoB).
- The terminal step is linked to energy conservation. In this step, the hetero-disulfide is reduced by F_{420} to regenerate the active form of coenzymes CoM-SH and CoB-SH. A hetero-disulfide reductase carries out this reduction. The reduction process is coupled to the pumping of protons across the membrane, generating a proton motive force and finally ATP is synthesized (Liu and Whitman, 2008).

The MCR is thus the key enzyme in this pathway and mediates the final step in methanogenesis; heterodisulfide formation between CoM and CoB with concomitant release of methane. The holoenzyme contains three subunits, which are encoded by the *mcr* operon (mcrABCDG) (Figure 2.). Methanogenic MCR is a 300 kDa heterotrimeric apocomplex with α2β2γ2 configuration. The active enzyme contains two binding sites that complex with two molecules of the 905 Da nickel porphyrin prosthetic group in F_{420} coenzyme (Ellefson and Wolfe, 1981, Ermler et al., 1997). The structure of the active site in the alph subunit in *Methanothermobacter marburgensis* is post-translationally modified involving thioglycineα445, N-methylhistidineα257, S-methylcysteineα452, 5-(S)-methylarginineα271 and 2-(S)-methylglutamineα400 (Ermler et al., 1997, Grabarse et al., 2000).

Figure 2. The mcrABCDG operon; the organization of the genes encoding the Mcr subunits in most species of methanogens and also in ANME-2c. Adapted from (Alvarado et al., 2014).

1.1.2. Anaerobic Oxidation of Methane (AOM)

1.1.2.1. Anaerobic Methanotrophic Archaea (ANME)

Anaerobic oxidation of methane, AOM, was first reported in marine sediments in 1976. Although the responsible microorganisms were not identified, AOM was reported to be coupled with sulfate reduction (Cui et al., 2015). Since then, extensive studies have been performed to identify the microorganisms catalyzing the process, their phylogeny and ecology as well as their biochemistry and energy conservation mechanisms (Callaghan, 2013, Cui et al., 2015, Knittel and Boetius, 2009).

Three clades, responsible for AOM, are known as anaerobic methanotrophic archaea (ANME) and are classified as ANME-1, ANME-2, and ANME-3 (Orphan et al., 2001, Knittel et al., 2005). The ANME are phylogenetically related to the methanogens (Figure 3.), but function as methanotrophs instead of methanogens and oxidize methane as an electron donor. Methane production has been only reported for ANME-1 (Lloyd et al., 2011). Based on the 16S rRNA, ANME-1 is distantly affiliated with *Methanosarcinales* and *Methanomicrobiales* and divided into two subgroups, ANME-1a and ANME-1b (Knittel et al., 2005).

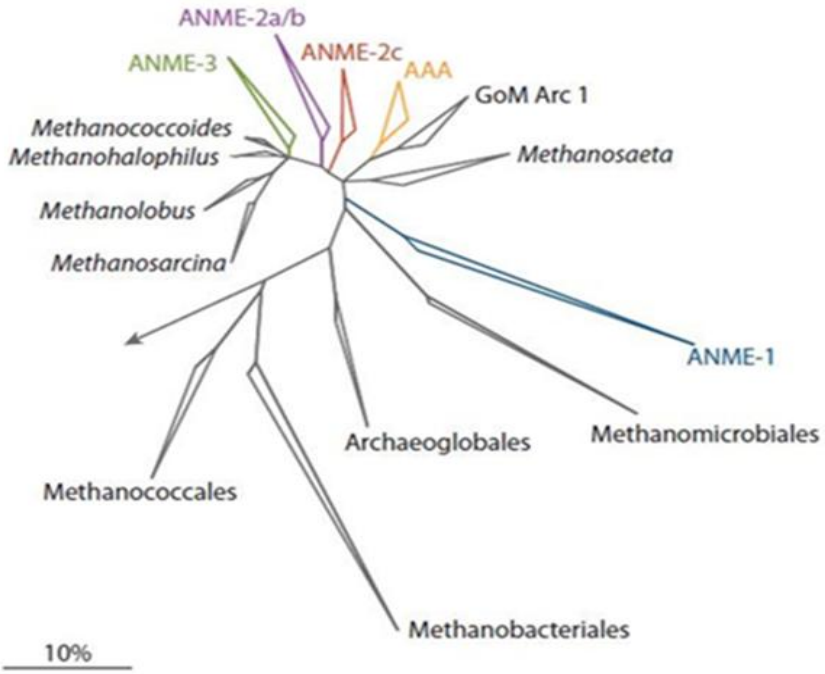

Figure 3. Phylogenetic relationship of ANME and methanogenes based on 16s rRNA gene sequences. ANME-2 and ANME-3 have close affiliation with *Methanosarcinales* and *Methanococcoides* respectively. ANME-1 is distantly related to *Methanosarcinales* and *Methanomicrobiales.* Adopted from (Knittel and Boetius, 2009).

ANME-2 belongs to *Methanosarcinales* (Knittel et al., 2005) and ANME-3 is related to the genera *Methanococcoides* (Niemann et al., 2006). Sequences affiliated with ANME-2 are classified into four distinct subgroups, designated ANME-2a, ANME-2b, ANME-2c, and ANME-2d (Figure 3.) (Mills et al., 2003, Orphan et al., 2001).

ANME are often found to co-occur with *Deltaproteobacteria* (Table 1.1.) in the AOM sites and AOM is suggested to be mediated through synthrophic consortia of ANME together with sulfate-

reducing bacterial partners, (SRB) (Knittel and Boetius, 2009). The process is catalyzed according to the overall reaction (Reaction 2) (Nauhaus et al., 2002).

$$CH_4 + SO_4^{2-} \rightarrow HCO_3^- + HS^- + H_2O \qquad (2)$$

ANME-1 and ANME-2 are shown to form consortia with SRB of the genera *Desulfosarcina–Desulfococcus* (DSS) (Boetius et al., 2000b, Orphan et al., 2002), whereas ANME-3 are associated with SRB of the genus *Desulfobulbus* (DBB) (Table 1.1.) (Niemann et al., 2006). Beside association of ANME with *Deltaproteobacteria*, association with other putative partners such as *Sphingomonas* spp. of *Alphaproteobacteria* and *Burkholderia* of *Betaproteobacteria*, has more recently been observed (Knittel and Boetius, 2009).

1.1.2.2. Reverse methanogenesis

The close phylogenetic relationship of ANMEs with methanogens are also reflected in their lipid structure, morphology/shape and by the presence of homologous genes for enzymes associated with the canonical seven-step methanogenic pathway (Figure 1. and Table 1.1.) (Cui et al., 2015, Hallam et al., 2004, Meyerdierks et al., 2010).

The studies of *mcr* genes retrieved from AOM habitats dominated by ANME-1 and ANME-2 populations, respectively, indicated highly conserved amino acid sequences and similar to the MCR involved in methanogenesis suggesting a fundamental role of MCR in reversed methanogenesis (Kruger et al., 2003, Knittel and Boetius, 2009). In 2004, in a metagenomic study by Hallam and colleagues (Hallam et al., 2004), genes encoding the reverse methanogenic pathways were found in fosmids of ANME. Later additional metagenomic and metaproteomic studies have supported that AOM occurs via the reverse methanogenesis pathway (Knittel and Boetius, 2009, Meyerdierks et al., 2005, Stokke et al., 2012). Notably, the enzyme N_5,N_{10}-methenyl-tetrahydromethanopterin reductase encoded by *mer* is detected in ANME-2 and -3 but is not found in ANME-1 (Hallam et al., 2004, Stokke et al., 2012, Knittel and Boetius, 2009). Interestingly, the ANME MCR- complex was found to be overall similar in structure to the methanogenic enzyme and contains Ni, CoM and CoB, however, it differs in some details by a different F_{420} variant and post-translational modifications (Shima et al., 2012).

1.1.2.2.1. Syntrophy and sulfate dependent AOM

Synthrophic AOM with sulfate requires an electron-shuttle from ANME to the sulfate-reducing partner and several different mechanisms have been proposed and tested. Electrons have been hypothesized to be shuttled as an organic compound such as formate, acetate, glucose, lactate, molecular hydrogen, carbon monoxide and redox-active small molecules including phenazines and humic acids (Nauhaus et al., 2005). However, some experimental evidences and modelling studies have discarded the putative role of hydrogen, formate, acetate or methanol as syntrophic intermediates for sulfate reduction during AOM (Meyerdierks et al., 2010, Moran et al., 2008).

Table 1.1. The properties of three groups of ANME, adapted from (Cui et al., 2015).

	ANME-1	ANME-2	ANME-3
Common features			
Habitat	Various anaerobic areas (marine sediments, cold seep, lake sediments, soils, oil field sediments, etc.)	Various anaerobic areas (marine sediments, cold seep, lake sediments, soils, oil field sediments, etc.)	Submarine mud volcanoes and marine methane seep
Subgroup	a, b	a, b, c, d	ND
Pure culture	No	No	No
Features associated with SRB			
Associated SRB	*Desulfosarcina* and *Desulfococcus*	*Desulfosarcina* and *Desulfococcus*	*Desulfobulbus*
Associated form	Often loose	Often form structured consortia	Often form structured consortia
Associated necessity	No	No	No
Single-cell form	Often	Yes	Yes
Features related to methanogens			
Related methanogen	*Methanosarcinales* and *Methanomicrobiales*	*Methanosarcinales*	*Methanococcoides*
Shape	Often rod shaped (like *Methanobacteriales* and *Methanomicrobiales*)	Often coccoid shaped (like *Methanosarcinales*)	Often coccoid shaped (like *Methanosarcinales*)
Harbour mcrA	Yes	Yes	Yes
mcrA subgroup	a, b (identified)	c, d (identified) e (possible)	f (identified)
Produce methane	Yes	ND	ND
Autofluorescent under UV light (like methanogens)	Yes	Yes	Yes

Meyerdierks and colleagues (Meyerdierks et al., 2010) identified a cluster of genes encoding putative secreted multiheme c-type cytochromes in their metagenomic and metatrascriptomic datasets of ANME-1, and based on this finding they suggested direct electron transfer from

ANME-1 to the bacterial sulfate-reducing partner via an extracellular conductive matrix (Meyerdierks et al., 2010).

Recently, another model has been proposed based on studies of an enrichment culture of consortia of ANME-2c and sulfate reducing bacteria (SRB) (Milucka et al., 2012). In this model, ANME is suggested to carry out both methane oxidation and sulfate reduction. Zero-valent sulfur is produced and disulfide is proposed as a key intermediate, taken up by the SRB (*Deltaproteobacteria*). This sulfur compound is subsequently disproportionated to sulfide and sulfate. The sulfate produced is reused in AOM by ANME (Figure 4.)(Reaction 3.). The expressed enzymes in the SRB, ATP sulfurylase (Sat) and dissimilatory sulfite reductase (Dsr), which are key enzymes in the canonical dissimilatory sulfate reduction pathway (Figure 4.) are suggested to rather take part in disulfide disproportionation. The mechanism for sulfate reduction by ANME was not identified and remains elusive.

$$7CH_{4\,(aq)} + 8\,SO_4^{2-} + 5\,H^+ \rightarrow 4HS^- + 7HCO_3^- + 11\,H_2O \qquad \Delta G = -26.5\,kJ\,mol^{-1}\,(CH_4) \qquad (3)$$

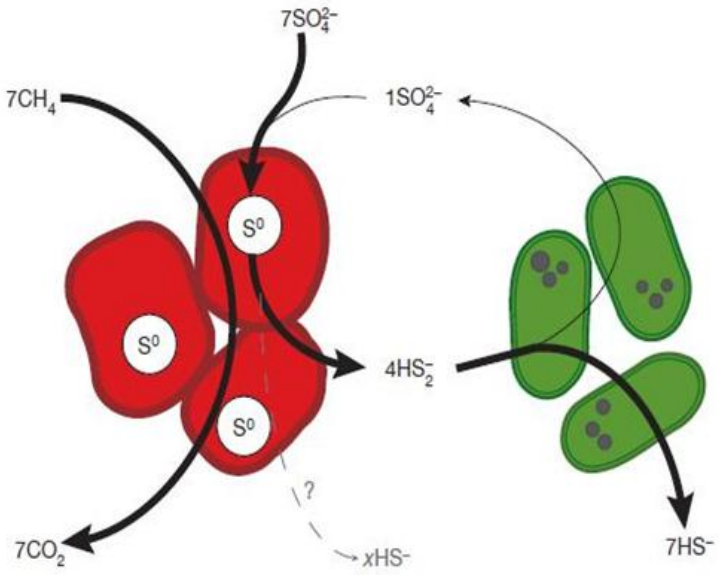

Figure 4. Schematic model of anaerobic oxidation of methane coupled to sulfate reduction in the consortia of ANME and SRBs. ANME (red) simultaneously, oxidize methane anaerobically and reduces sulfate to zero-valent sulfur (S^0, elemental sulfur) . Elemental sulfur reacts with sulfide and forms polysulfides. *Deltaproteobacteria* takes up the polysulfide and produce sulfate and sulfide through sulfate disproportionation. The produced sulfate may be re-used by the ANME, adapted from (Milucka et al., 2012).

1.1.2.2.2. Nitrate/Nitrite-Dependent AOM

Nitrate/nitrite-dependent AOM (Reaction 4. and Reaction 5.) has recently been described (Ettwig et al., 2010, Haroon et al., 2013b). So far, it has been reported only in different natural freshwater habitats (Cui et al., 2015).

$$5CH_4 + 8NO_3^- + 8H^+ \rightarrow 5CO_2 + 4N_2 + 14H_2O \qquad \Delta G^0 = -765\ kJmol^-\ CH_4 \qquad (4)$$

$$3CH_4 + 8NO_2^- + 8H^+ \rightarrow 3CO_2 + 4\,N_2 + 10H_2O \qquad \Delta G^0 = -928\ kJmol^-\ CH_4 \qquad (5)$$

Based on the genomic studies on *Candidatus* Methylomirabilis oxyfera an intra-aerobic" pathway of nitrite reduction was found (Ettwig et al., 2010). A disproportionation of NO_2^- into NO and O_2 provides O_2 for methane oxidation, a mechanism that allows *Candidatus Methylomirabilis oxyfera,* to couple AOM to nitrite reduction without the aid of any other partner.

Reconstruction of a genome of ANME-2d, based on metagenomic data, identified genes for nitrate reduction as well as the genes encoding a complete reverse methanogenesis pathway (Haroon et al., 2013). This ANME-2d was termed *Candidatus* Methanoperedens nitroreducens (Haroon et al., 2013a). Despite these hypotheses, the mechanism of AOM coupled to nitrate/nitrite reduction is still ambiguous.

1.1.2.2.3. Metal Ion (Mn4+ and Fe3+)-Dependent Anaerobic oxidation of Methane

In this process, methane oxidation is coupled with the reduction of metal ions such as (Mn^{4+}) and iron (Fe^{3+}). The mechanism and the microorganisms involved in this process are still unknown; however, ANME-1 and ANME-2, and An uncultivated group, affiliated with the marine benthic group D were dominant in the sediment where metal ion reduction seems to be coupled to AOM (Beal et al., 2009).

1.2. Dissimilative Sulfate reduction

Oxidized sulfur compounds including sulfate, elemental sulfur and thiosulfate are common electron acceptors that are available in the dark ocean (Orcutt et al., 2011). Sulfate (SO_4^{2-}), the most oxidized form of sulfur, is one of the most abundant anions in seawater and participates in anaerobic respiration reactions as an electron sink (Orcutt et al., 2011). It is utilized either as a sulfur source for biosynthetic reactions (known as assimilative sulfate reduction) or as an electron acceptor through energy-generating process (known as dissimilative sulfate reduction) (Madigan et al., 2015). Assimilative sulfate reduction is widespread in many organisms such as plants, algae, fungi, and most prokaryotes whereas reduction of sulfate through the dissimilative sulfate reduction is restricted to a small fraction of prokaryotes population (Hansen, 1994, Madigan et al., 2015). Sulfate-reducing prokaryotes comprising both bacteria and archaea play a key role in anaerobic degradation in presence and even absence of sulfate, and are able to utilize a wide range of substrates such as fermentation products and intermediate breakdown products e.g. certain amino acids, glycerol, and fatty acids as well as H_2 (Hansen, 1994). Almost all species of sulfate-reducing bacteria use Hydrogen as electron donors whereas this is not the case for other electron donors. For example marine sulfate-reducing bacteria utilize acetate and longer-chain fatty acids and species found in freshwater anoxic environments prefer lactate and pyruvate. Some species, such as *Desulfosarcina* and *Desulfonema,* grow chemolithotrophically and utilize H_2 as an electron donor, SO_4^{2-} as an electron acceptor, and CO_2 as the sole carbon source. In organotrophic sulfate reducers, such as *Desulfovibrio* species, organic compounds e.g. lactate, pyruvate, or ethanol are oxidized to acetate with the production of hydrogen (Madigan et al., 2011).

So far, isolation and characterization of any SRB partner of ANME, has not been successful and whether they are dependent on a true syntrophic relation or not remains unknown. However, the model by Milucka et al, may hint to a lifestyle including disproportionation of sulfur compounds (Milucka et al., 2012).

In both assimilative and dissimilative reactions, the product is hydrogen sulfide (Figure 5.). Produced H_2S through dissimilative reduction is excreted from the cell and is available for other organisms or it is free to react with other elements, such as metals. In contrast, hydrogen sulfide resulted in the assimilative reduction of sulfate is assimilated into organic sulfur compounds such as sulfur-containing amino acids (Madigan et al., 2015).

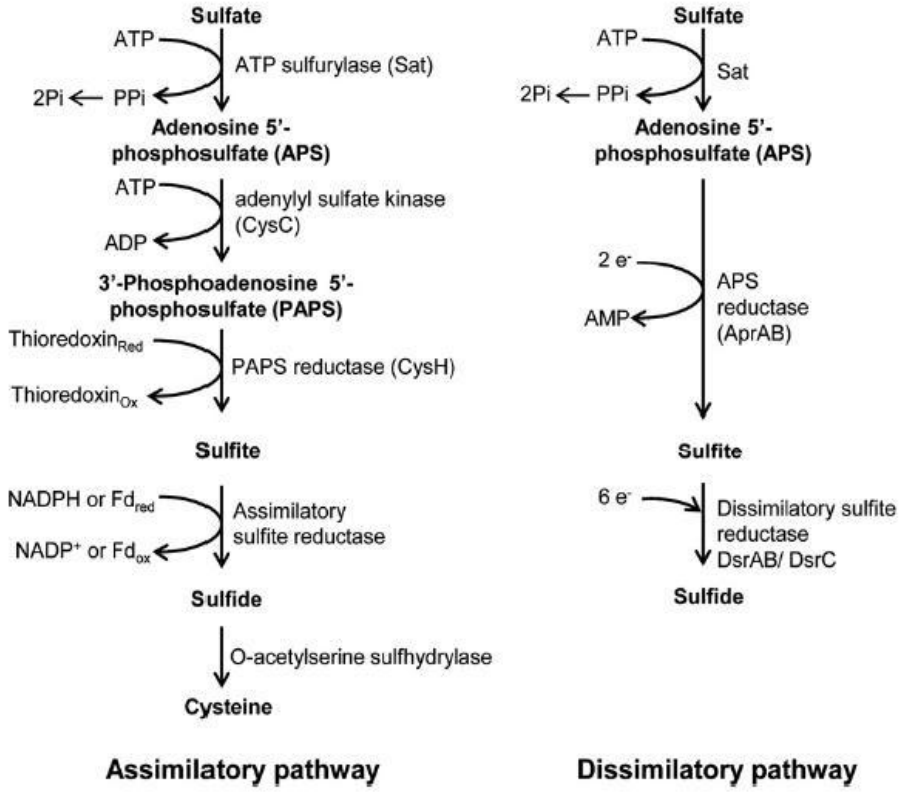

Figure 5.Assimilatory and dissimilatory sulfate reduction pathways. Both of these pathways initiate with activation of sulfate by reacting with ATP. Adenosine 5'-phosphosulfate (APS) is reduced to sulfite and finally to sulfide. Dissimilatory sulfate reduction costs 1 ATP, whereas assimilatory sulfate reduction costs 2 ATPs. Adopted from (Grein et al., 2013).

The first step of both pathways includes activation of stable molecule of sulfate by reacting with ATP catalyzed by Sulfate adenylyltransferase, known as Sat. This enzyme catalyzes the transfer of the adenylyl group from ATP to inorganic sulfate, forming adenosine 5'-phosphosulfate (APS) and pyrophosphate (Hansen, 1994, Taguchi et al., 2004, H. D. PECK, 1962). During the prokaryotic assimilatory pathway APS is converted to 3′-phosphoadenosine-5′-phosphosulfate (PAPS). Subsequently PAPS is reduced to sulfite, and finally sulfite is reduced to sulfide (Crane and Getzoff, 1996, Madigan et al., 2015). In the dissimilatory pathway APS is reduced to sulfite by the APS reductase (Apr). Then sulfite is reduced to sulfide by dissimilatory sulfite reductase (Dsr) (Madigan et al., 2015).

Aps reductase is a αβ heterodimeric iron-sulfur flavoenzyme (Grein et al., 2013). The AprA subunit contains an FAD group whereas AprB subunit contains two [4Fe-4S] 2+/1+ clusters. Despite low sequence identity, the structure of the AprA is strongly similar to the family of flavoproteins such as fumarate reductase and aspartate oxidase. The AprB subunit contains the bacterial ferredoxin-like domain (Fritz et al., 2002). The reduction of sulfite to sulfide is catalyzed by a multi-meric dissimilatory sulfite-reductase DsrABC. DsrD is a small protein that is thought to have regulatory role in sulfite reduction (Caffrey and Voordouw, 2010, Mizuno et al., 2003). The DsrAB sulfite reductase forms a $\alpha_2\beta_2$ unit. Each αβ unit contains siroheme cofactors, coupled to a [4Fe\4S] iron–sulfur cluster through the cysteine heme axial ligand. In active DsrAB, only one of the cofactors is catalytically active (Oliveira et al., 2008).

It has been proposed that either intracellular or extracellular hydrogen cycling involve in the energy conservation in sulfate respiration (Keller and Wall, 2011, Ramos et al., 2012). The internal hydrogen can be produced from the catabolism of organic compounds such as lactate and pyruvate, and across the cytoplasmic membrane into periplasmic space. Either the internal produced hydrogen or external hydrogen is oxidized by the periplasmic hydrogenase to electrons and protons. Generated protons gradually establish the proton motive force for ATP synthesis by ATPase. During dissimilative sulfate reduction eight electrons are transferred through a number of intermediate transport reactions leading to a proton motive force and gradually ATP synthesis by ATPase. Cytochrome c_3 plays major role in transferring electrons from periplasmic hydrogenase to a membrane-associated protein complex, known as Hmc (Madigan et al., 2015) (Figure 6.).

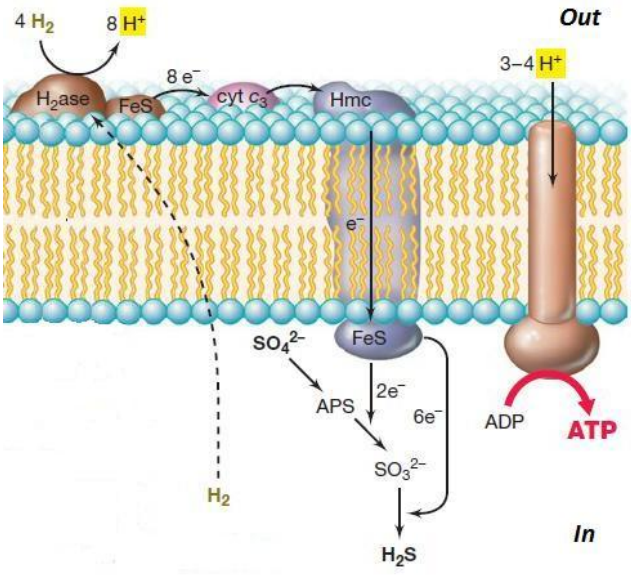

Figure 6. Electron transport and energy conservation in sulfate-reducing bacteria. H_2 with either external or internal origin is oxidized by the periplasmic hydrogenase to electrons and protons. The periplasmic cytochrome (cyt) c3, and a cytochrome complex (Hmc) transfer electrons to a transmembrane protein by which electrons are shuttled across the cytoplasmic membrane and delivered to the Apr and Dsr enzyme complexes. ATP is synthesized through the proton motive force by ATPase. Adopted from (Madigan et al., 2011).

The electrons are transferred trough the membrane via the Qmo and DsrMKJOP complexes to the AprAB and Dsr respectively. Qmo is composed of three subunits A,B and C in which QmoA and QmoB are cytoplasmic and QmoC is membrane-bound (Grein et al., 2013). The QmoC

subunit constitutes a cytochrome b transmembrane domain and a hydrophilic cytoplasmic domain containing two [4Fe\4S] cluster binding sites. The cytochrome b domain facilitates the electron flow between the quinone pool and the cytoplasm (Grein et al., 2013, Ramos et al., 2012). The QmoA and QmoB subunits are both flavoproteins (Grein et al., 2013). The direct protein-protein interaction between QmoABC and AprAB was also reported in *Desulfovibrio spp*, (Ramos et al., 2012). DsrMKJOP is a multimeric transmembrane complex shuttling the electrons across the membrane to Dsr. DsrMKJOP complex constitutes of two periplasmic subunits: DsrJ and DsrO, two integral membrane subunits: DsrM and DsrP, and a cytoplasmic subunit ,DsrK (Grein et al., 2013). The DsrMKJOP complex appears to be a combination of two sub-complexes: the DsrMK and the DsrJOP subunits in which the DsrJOP module possibly, involved in electron swap between the periplasm and the quinone pool, and DsrMK between the membrane pool and the cytoplasm. Although there are some evidences that the complex seems to function as a complete unit (Grein et al., 2013).

1.3. Carbon fixation

Access to the carbon source is one of the cornerstones of life formation. Organisms are classified into autotrophs and heterotrophs based on their ability to build all cell material solely from inorganic carbon present in their surroundings. Autotrophs utilize energy from either light (photoautotrophs) or inorganic chemical reactions (chemolitotrophs) and fix inorganic carbon e.g. CO_2, CO into organic compounds for biosynthesis and also create a store of chemical energy. Carbon dioxide, CO_2, is one of the most common inorganic carbon sources in nature. So far, six autotrophic pathways have been discovered including the Reductive pentose phosphate (Calvin-Benson) cycle, Reductive Acetyl-CoA (Wood-Ljungdahl) pathway, Reductive citric acid (Arnon-Buchanan) cycle, Dicarboxylate/4-hydroxybutyrate cycle, 3-Hydroxypropionate/4-hydroxybutyrate cycle and 3-hydroxypropionate bi-cycle (Fuchs, 2011, Hugler and Sievert, 2011).

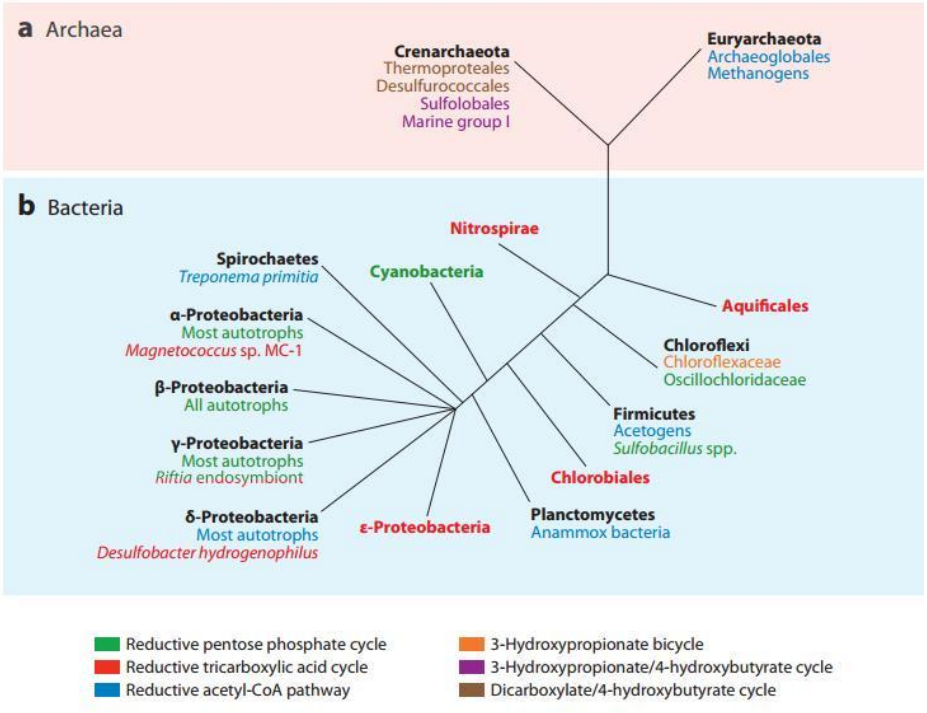

Figure 7. The phylogenetic distribution of the carbon fixation pathways. Adopted from (Hugler and Sievert, 2011).

Since this study attempts to address the functional potential of the microorganisms involved in the Nyegga region i.e. ANME and *Deltaproteobacteria*, we present two alternative pathways which are used by sulfate reducing bacteria (SRBs) and methanogens (Figure 7.) (Hugler and Sievert, 2011).

1.3.1. Wood-Ljungdahl pathway

The acetyl-CoA pathway, also known as the Wood-Ljungdahl pathway is widely used by acetogenic bacteria and other *Eubacteria* and some *Euryarchaeota* (Ljungdahl, 1986, Wood, 1991). Sulfate-reducing bacteria and methanogens are among the organisms that employ the reductive acetyl-CoA pathway for autotrophic purposes and reduce CO_2 to acetate and utilize it as a source of cell carbon for cell biosynthesis.

The acetyl-CoA pathway is the only autotrophic pathway that is not a cycle and can simultaneously fix CO_2 and synthesize ATP by converting acetyl-CoA to acetate. It includes two linear pathways. Through one of these pathways requiring the coenzyme tetrahydrofolate, one molecule of CO_2 is reduced to the methyl group and remains bound to a tetrahydropetrin. The other molecule of CO_2 is reduced to the carbonyl group through the other reaction, which is catalyzed by carbon monoxide (CO) dehydrogenase (Figure 8.). This is the key enzyme of acetyl-CoA pathway and contains Ni, Zn and Fe as cofactors. Finally combination of CO and CH_3 groups with CoA results in acetyl-CoA (Madigan et al., 2015, Fuchs, 2011, Hugler and Sievert, 2011).

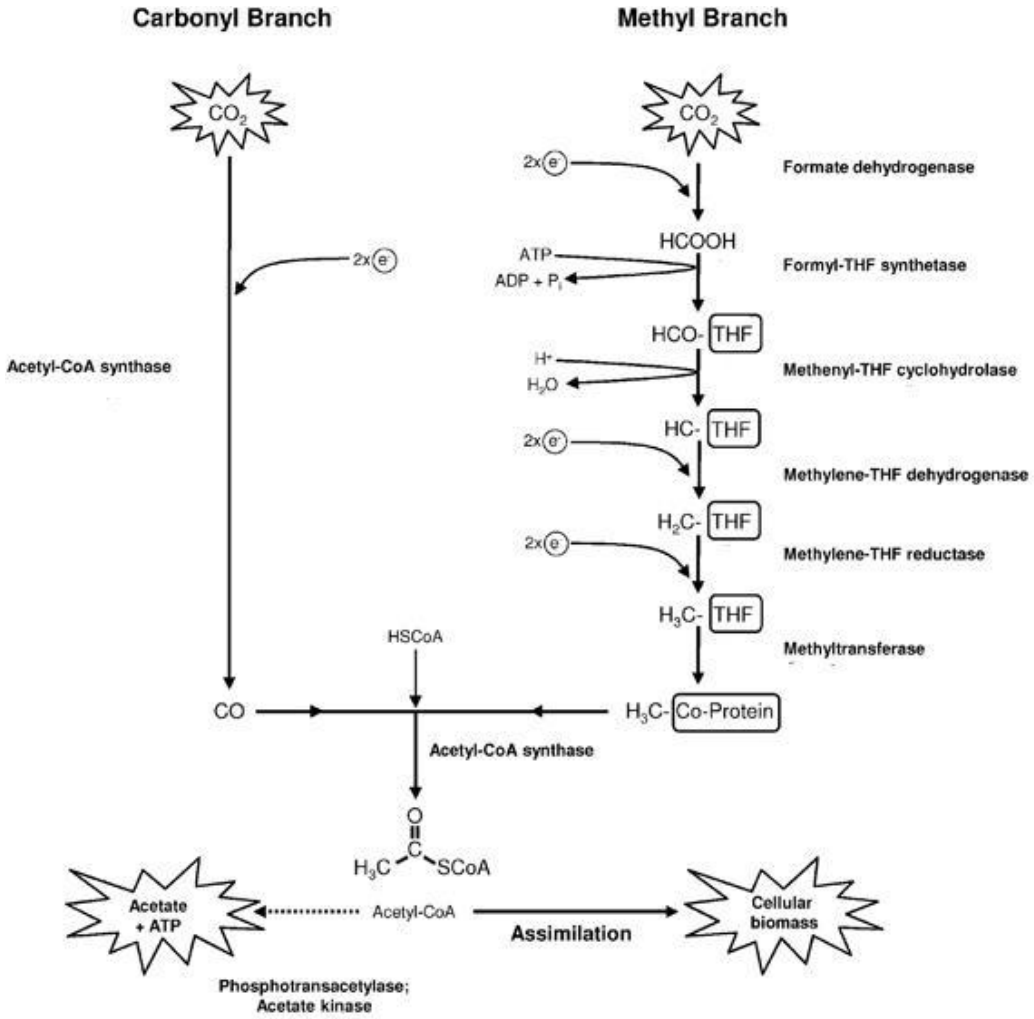

Figure 8. Acetyl-CoA pathway. The reduction of CO_2 along two linear pathways; one molecule of CO_2 is reduced to the methyl group of acetate, and the other molecule of CO_2 is reduced to the carbonyl group. The two C1 units are then combined at the end to form acetyl-CoA, adopted from (Siegl et al., 2011).

1.3.2. Reductive citric acid cycle

The reductive citric acid cycle, also known as Arnon-Buchanan, is employed by various groups of strict anaerobic (Aoshima, 2007) and even microaerobic Eubacteria (Hugler and Sievert, 2011). The presence of this cycle also has been reported in *Desulfobacter hydrogenophilus* (Schauder et al., 1987).

This cycle is a reversal of the oxidative citric acid cycle (TCA or Krebs cycle) (Figure 9.) i.e. instead of oxidizing acetyl-CoA that is performed in heterotrophic organisms for ATP synthesis; it is used for the biosynthesis of acetyl-CoA from two molecules of CO_2 (Fuchs, 2011). Most of the enzymes such as Malate dehydrogenase, Fumarate hydratase, Succinyl-CoA synthetase, Isocitrate dehydrogenase, Aconitate hydratase, are common in the oxidative and reductive TCA cycle; the difference is the direction in which the reactions operate. However, the enzymes involved in irreversible steps are replaced for reductive direction constituting the key enzymes of the reductive TCA cycle e.g. Fumarate reductase, Ferredoxin-dependent 2-Oxoglutarate synthase (2-Oxoglutarate:ferredoxin oxidoreductase) and ATP citrate lyase (Fuchs, 2011, Hugler and Sievert, 2011). The reductive TCA cycle operates in an energetically unfavorable direction (Fuchs, 2011). Two carboxylation reactions are accomplished in this cycle; first the reductive carboxylation of succinyl-CoA to 2-oxoglutarate and second the reductive carboxylation of 2-oxoglutarate to isocitrate. The key reaction of the rTCA cycle is the ATP-dependent cleavage of citrate to acetyl-CoA and oxaloacetate by ATP citrate lyase (Fuchs, 2011, Hugler and Sievert, 2011).

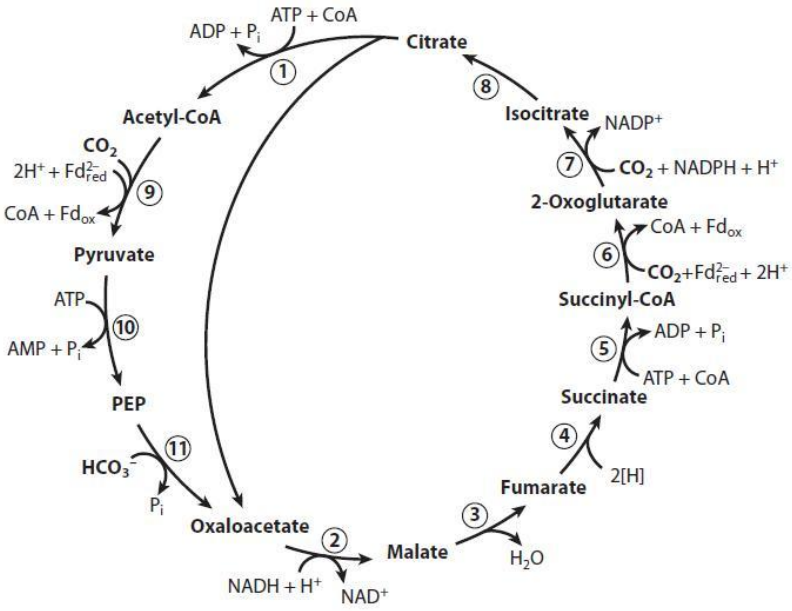

Figure 9. Reductive citric acid cycle. The enzymes involved in this cylces are: 1) Malate dehydrogenase (NADH), 2) Fumarate hydratase, 3) Fumarate reductase, 4) Succinyl-CoA synthetase (ATP-dependent), 5) 2-Oxoglutarate synthase (Fd2− red), 6) Isocitrate dehydrogenase [NAD(P)H], 7) Aconitase, 8) ATP-citratelyase, 9) Pyruvate synthase (Fd^{2-}_{red}), 10) Pyruvate:water dikinase and 11) PEP carboxylase. The produced acetyl-CoA can be used in either biosynthetic processes or energy generating process. Adopted from (Fuchs, 2011).

1.4. Nitrogen fixation

Ammonia is the major form of the fixed nitrogen, which is ready for assimilation into organic forms such as amino acids and nucleotides. However, it is not available in all habitats. The biological process, in which dinitrogen (N_2) is enzymatically reduced to the form of compounds that can be used as nutrients, is called nitrogen fixation or diazotrophy (Madigan et al., 2015). It provides a source of nitrogen to the majority of the biosphere that cannot directly assimilate molecular nitrogen (N_2). The diazotrophy is a practical strategy to overcome nitrogen limitation, specifically in the habitats where host organisms that derive carbon primarily from nitrogen-depleted sources, such as CO_2 (e.g. cyanobacteria and plants) and CH_4 (e.g. anaerobic methanotrophic bacteria) (Dekas et al., 2014). Only certain prokaryotes including bacteria and the archaea can fix nitrogen. Some are free-living whereas others are associative symbioses and fix nitrogen only in association with certain host such as plants (Madigan et al., 2015). Although most of the bacterial phylogenetic groups, including green sulfur bacteria, Firmibacteria, actinomycetes, cyanobacteria and all subdivisions of the Proteobacteria are able to fix nitrogen, but in archaea, nitrogen fixation is mainly restricted to methanogens. The diazotrophy has been reported in a diazotrophic methanogen from hydrothermal vent fluid near the Juan de Fuca Ridge and ANME-2 at Eel River Basin (Dekas et al., 2009).

Diazotrophy is catalyzed by a large enzyme complex, nitrogenase, consisting of two distinct proteins, dinitrogenase and dinitrogenase reductase. Both proteins contain iron, and dinitrogenase contains molybdenum in addition. Dinitrogenase consists of a cofactor called the iron–molybdenum cofactor, in which the actual reduction of N_2 occurs. The activation and reduction of nitrogen molecule requires six electrons and is highly energy demanding process, due to the stability of the triple bond in N_2. The electrons are transferred from the electron donors (e.g. ferredoxin or flavodoxin) to dinitrogenase reductase and then to dinitrogenase to reduce N_2. Despite some differences, diazotrophy in methanogens operated with the same basic mechanism (Leigh, 2000).

In methanogens, the proteins involved in nitrogen fixation are encoded by nif operon consisting of six nif genes (Figure 10.). The nifK and nifD encode for the beta and alpha subunits of denitrogenase respectively, whereas nifH encode the denitrogenase reductase. The bacterial and the archaeal sequences of these genes are clear homologues and the nif gene organization is so conserved among the methanogens (Leigh, 2000). The nifE and nifN encode proteins responsible for formation of a functional catalytic site of the nitrogenase. The nif genes are present as a single operon in methanogens whereas in bacteria the nif genes are organized in nif regulon consisting several operons (Leigh, 2000).

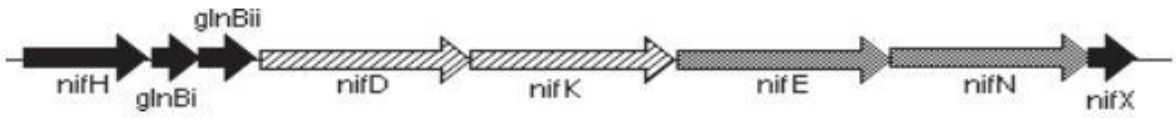

Figure 10. The organization of nif genes in methanogens. Adopted form (Leigh, 2000).

1.5. Metagenomic study

Classic microbial ecology has relied on characterization and categorization of cultured micro-organisms. However, the development of culture-independent molecular methods has had a tremendous impact on microbial ecology and allowed researchers to address two main questions "Who is there?" and "What are they doing there?"(Handelsman, 2004). It was shown that rRNA genes can be used as evolutionary chronometer in population monitoring. It provides information about the taxonomic composition and phylogenetic structure of a microbial community (Woese, 1987).

Metagenomics refers to the comprehensive study of a collection of genetic material, constituting various genomes from a mixed community. As indicated by the Greek preposition 'meta', metagenomic studies target the identification of the total biological entities within a complex instead of the characterization of the single species (Zepeda Mendoza et al., 2015). Metagenomic not only circumvents culturing the organisms under study but also provides the phylogenetic properties of the environmental niche itself, and it can give an overview of its transcripts composition and the potential physiology of the abundant community members. This information provides us with a recipe to recreate or redesign microbial pathways, and even a part of the system *in vitro* (Ladoukakis et al., 2014). The effective bioinformatic pipeline for analysis of a metagenomic sample should cover certain successive tasks in order to extract information from the huge volume of short sequence reads and to result in a comprehensive and accurate assessment. It constitutes: (i) DNA extraction and DNA sequencing (ii) assembly, (iii) gene detection and gene annotation, (iv) taxonomic analysis, and (v) comparative analysis (Ladoukakis et al., 2014).

Several methods exist to determine the accurate order of nucleotides within a DNA molecule. The Sanger conventional DNA sequencing relies on the principle of the dideoxy chain termination technique (Sanger et al., 1977). Despite major improvements during the years, limitations in throughput, scalability, speed, resolution, and cost have restricted the application of this technique. The inventions of Next-Generation sequencing technologies such as 454-pyrosequencing (Ronaghi et al., 1998), Illumina (Bentley et al., 2008) and IonTorrent (Rusk, 2011) have helped the scientists to overcome these barriers and decipher ambiguities in biological systems. Rapid developments in high-throughput sequencing (HTS) technologies have had a major impact on metagenomics analysis. Low costs and ease of these technologies have facilitated the possibility of studying wide range of samples from the human gut to environmental samples such as Antarctic lakes and hot springs (Ladoukakis et al., 2014).

DNA sequencing technology cannot read whole genomes in one go and results in small pieces of DNA sequences, reads, between 20 and 30000 bases, depending on the technology used. There are two main computational approaches for assembly of the Next Generation Sequencing (NGS) data: mapping reads to a template genome and de novo. Through mapping approach, reads are mapped based on the reference genome, which is phylogenetically related to the sequenced

sample (Scheibye-Alsing et al., 2009). De novo assembly, also known as overlay-layout-consensus (OLC), relies on algorithms that perform all possible comparisons between the millions of reads to find any overlaps between them (Zerbino and Birney, 2008). Although this approach is a very intensive computational task since the reference genome is not always available and because of the presence of the immense diversity of the genomic content in metagenomics studies, de novo assembly is the sole alternative approach.

Since DNA extraction from metagenomic samples constitutes various genomes from a mixed community, it is impossible to separate and segregate DNA sequences before the DNA collection according to the microorganism they originated from. Nonetheless, this challenge may be addressed computationally through binning, in which contigs or reads that seem to arise from the same source of population, are clustered (Strous et al., 2012b). The proposed approaches for the binning problem can be divided into two groups; those that rely on similarity-based methods, such as BLAST (Huson et al., 2011) and hidden Markov models, and the compositional-based approaches such as tetra nucleotide frequencies, interpolated Markov models and Markov chain Monte Carlo models (Ladoukakis et al., 2014, Strous et al., 2012a). The similarity-based methods are very robust specifically in grouping the contigs with sufficient length. (Strous et al., 2012b). Compositional approaches are able to cluster the contigs harboring the genes that are not homologous to the reference species. (Strous et al., 2012b).

There are several pipelines for automatically processing metagenomic dataset and integrating tools in the form of services such as CloVR metagenomics (Angiuoli et al., 2011), IMG/M (Markowitz et al., 2014) and RAST (Aziz et al., 2008).

2. Aim of the study

Anaerobic methanotrophic archaea (ANME) play an important role in marine methane-rich sediment where they consume a substantial fraction of the methane rising from sub-surface reservoirs. Although AOM coupled to sulfate reduction was discovered about three decades ago, the exact nature of the process is still poorly understood. According to previous metagenomic-based analyses, methane oxidation is likely mediated by the symbiosis of ANME and SRBs via reverse methanogenesis but it still remains unresolved what kind of electron transport components and knowledge on energy conservation mechanisms mediate this process. In addition for the co-occurring *Deltaproteobacteria*, there is currently no information available on their metabolic flexibility (substrate), CO_2 fixation pathways and on energy conservation mechanisms.

The aim of this study was to obtain genome information of ANME-2c and its bacterial partner to learn more about the energy metabolism of putative key players taking part in AOM in general and specifically in the Nyegga cold seeps. The Nyegga cold-seeps have been subjected to several multidisciplinary geological studies and the microbial community structures have been identified, however the functional potential of this site has not been completely studied.

The following sub-goals were set:

- Identify genes encoding the major metabolic pathways for AOM.
- Identify pathways involved in energy generation and biosynthesis e.g. CO_2 and nitrogen fixation.

3. Experimental procedures

3.1. Sampling site

A push core sample (08ROV29) was collected from sediments the G11 pockmark in Nyegga (64°39.788'N; 05°17.317'E) in 2008 (Roalkvam et al., 2011). The Argus Bathysaurus remote operating vehicle system on the research vessel G.O.Sars was used for core sampling. Nyegga is located on the mid-Norwegian continental slope at ~730 meters water depth. From the south, it is surrounded by the Storegga Slide and Møre basins and by the Vøring Basin from the north (Hovland et al., 2005, Ivanov et al., 2010).

Methane-enriched fluids emit vertically over time from Nyegga pockmarks, where the source is deeper thermogenic methane from gas hydrates and biogenic methane formed during the advection towards the sediments surface (Mazzini et al., 2006). Although a constant stream of gas bubbles is not visible in the G11 pockmark, the gas hydrates form a reservoir of methane in the sediment horizon below ~75-100 cm below seafloor (cmbsf).

3.2. DNA isolation

Total DNA was extracted by Dr. Irene Roalkvam from the push core, 08ROV29, from the sediment horizon at 20-22 (cmbsf). The sediments were stored at -80°C, and in total 4.661gr was used in 4 parallel DNA extractions (approximately 1 gr for each extraction). The RNA PowerSoil® total RNA isolation kit and RNA PowerSoil® DNA Elution Accessory kit supplied by MOBIO laboratories were used to first extract the RNA and then the DNA, following the kit protocols. The DNA in each sample was eluted in 60 µl elution buffer supplied by the kit. The Amicon® Ultra-0.5 Centrifugal Filter Devices (Merck Millipore) was used to concentrate the DNA. All the four samples were loaded on one column and centrifuged at 14.000xg for 5 min to remove the excess buffer. Then the column was centrifuged at 1000xg for 2 min to elute the DNA. Finally 24µl of DNA sample was obtained. The concentration of DNA was measured by $A_{260/280}$ ratio measurements using a Cary 300 Bio UV–Vis Spectrophotometer (Varian Inc., Palo Alto, CA). The final concentration of DNA was 48.39ng/µl. In total 1.161µg DNA was sent for sequencing.

3.3. Sequencing

The DNA was subjected to 454-pyrosequencing by the GS-FLX Titanium system at the Norwegian Sequencing Centre (https://www.sequencing.uio.no). The pyrosequencing method was developed by Pål Nyrén and Mostafa Ronaghi and relies on the sequencing by synthesis principle where a single strand of the DNA (ssDNA) is sequenced along the synthesis of its complementary strand (Ronaghi et al., 1998). Incorporation of a nucleotide into the growing strand leads to the release of pyrophosphate, which is detected by light emission as a result of luciferase activity. The major steps in 454-pyrosequencing was reviewed by Mardis (Mardis, 2008) and is presented in Figure 11.

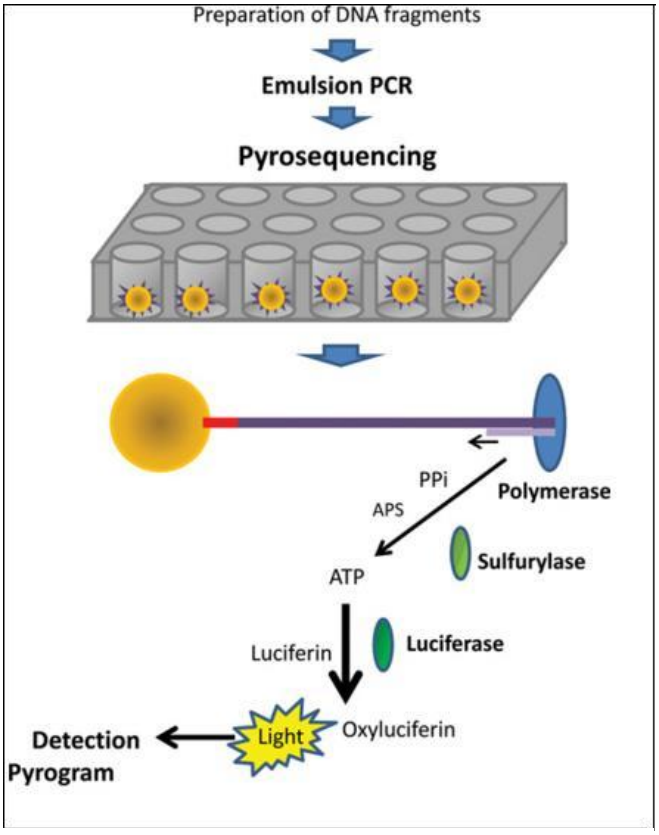

Figure 11.The major pyrosequencing steps. The genomic library is first fragmented and tagged with the adaptor sequences. The next step is the emulsion PCR in which clonal amplification occurs inside the micelles containing the fragment: bead. The beads are arrayed into a picotiter plate and are ready for sequencing. Incorporation of a nucleotide into the growing strand leads to the release of pyrophosphate, which is used by ATP sulfurylase. The produced ATP is up taken by Luciferase. Finally the light emission as a result of luciferase activity is detected. Adopted from (Siqueira et al., 2012).

The first step after DNA extraction and purification is the library fragmentation in which the genomic DNA is randomly sheared into short segments. These fragments are tagged with adapters on either side of the cut points. The adaptors are short DNA sequences used in the subsequent purification, quantification, amplification and sequencing steps. The tagged fragments are mixed with a population of agarose beads whose surfaces carry oligonucleotides complementary to the 454-specific adapter sequences on the fragment library. The ssDNA anneal the complementary oligos, so each bead is associated with a single fragment. The next step is the emulsion PCR in which each of the fragment: bead complexes are isolated into individual oil:water micelles that also contain PCR reactants. During the thermal cycling, clonal amplification occurs inside the micelles where each bead gets coated by approximately one million copies of the DNA fragments. The beads are arrayed into a picotiter plate with several hundred thousand wells, with a single bead in each well. Therefore, the ssDNA template is immobilized in the picotiter plate well. All the requirements for catalyzing the downstream pyrosequencing reaction steps are added into the wells (Mardis, 2008, Ronaghi et al., 1998).

The ssDNA template is hybridized to a sequencing primer, and the sequencing occurs in the presence of the enzymes DNA polymerase, ATP sulfurylase, luciferase and apyrase, and the substrates adenosine 5´- phosphosulfate (APS) and luciferin. The addition of one of the four deoxynucleoside triphosphates (dNTPs) initiates the DNA synthesis if the complementary nucleotide is available on the template strand. DNA polymerase incorporates the correct, deoxy nucleotide (dNTP) into the template, which releases pyrophosphate (PPi). ATP sulfurylase catalyzes the conversion of PPi to ATP in the presence of adenosine 5´- phosphosulfate. Luciferase converts luciferin to oxyluciferin and visible light in the presence ATP. The intensity

in of the light is proportional to the amount of ATP. Finally, a pyrase degrades the unincorporated nucleotides and ATP, and the reaction is restarted with another dNTP (Ronaghi et al., 1998).

3.4. Assembly

All sequencing methods provide data in the form of short nucleotide sequences, known as reads. The reads represent amplified sections of DNA molecules, due to the shearing of DNA prior to the shotgun sequencing. Assembly is a critical step of any genome analysis, whether the data corresponds to single cell genomes or metagenomic samples (Miller et al., 2010). It refers to recreating the original sequence through aligning and merging of the reads to a set of contiguous coherent sequence (contig) constructs. It is also possible to construct super-contigs, also known as scaffolds, containing multiple contigs with the reliable connection between them (Miller et al., 2010). The 454 GS FLX Titanium chemistry used in the sequencing of the DNA in this project produces reads with 400-500 base pair (bp) read lengths. One full plate was used in this project, which should give approximately 1,000,000 reads in one run. Reads were assembled by Dr. Runar Stokke using Newbler v2.5.3 provided by 454 Life Sciences/Roche with 98% identity and 50 bp overlap as assembly criteria. Filtering of poor-quality sequences, repeats and to short reads was processed as implemented in the Newbler software.

3.5. Metagenomic binning

DNA extracted from environmental samples constitutes multiple genomes from a mixed community. Metagenomic binning refers to the clustering of assembled DNA contig/scaffold sequences for microbial physiology of mixed cultures using computational approaches. The proposed approaches for the binning problem can be divided into two groups: those that rely on homology-based methods, such as Megan (Huson et al., 2011) and hidden Markov models; and the composition-based approaches, such as tetra nucleotide frequencies, interpolated Markov models and Markov chain Monte Carlo models (Ladoukakis et al., 2014, Strous et al., 2012b).

In this project the assembled contigs were clustered using the composition-based MetaWatt Binner version 3.2. (Strous et al., 2012a). The MetaWatt Binner uses an unsupervised (comparison of the metagenomic contigs only to each other) method based on multivariate statistics of tetranucleotide frequencies, differential coverage and read mapping information to bin assembled contigs. Taxonomic classification in MetaWatt is performed by diamond blastx against a database of reference genome sequences downloaded from NCBI (http://www.ncbi.nlm.nih.gov/). The module for taxonomic classification in MetaWatt is described in the manual by fragmenting each contig down into 1000 bp size. These fragments are blasted separately against the database. The contig blast results are analyzed as follows: (1) The number of top-scoring hits for each reference taxon is counted for each contig, (2) when binning is performed, the counts are added for each taxon for all contigs in the bin, (3) results are displayed as a pie diagram for each bin. The diagram indicates the counts of the top-scoring taxa as a percentage of the total number of fragments generated.

The three major MetaWatt bins were imported into RAST for further metabolic analysis.

3.6. Open reading frame (ORFs) detection and gene annotation

There are two groups of software for gene detection; the *ab initio* programs and similarity-based programs. *Ab initio* programs such as GENIE and GENEID (Yok and Rosen, 2010) recruit a training set with known annotation to define the parameters of their models to predict genes. The similarity-based programs utilize the external information of known sequences to predict genes. The well-known algorithm in this group is BLAST (Altschul et al., 1990, Mount, 2007, States and Gish, 1994) that searches the query sequence against a database of known protein sequences. The putative genes are translated to into functional proteins i.e. regarding the sequence length, and should begin with a start codon and end with an in-frame stop codon.

In this study, open reading frames (ORFs) in assembled contigs were predicted by Dr. Runar Stokke, using the software Prodigal v.60 (Hyatt et al., 2010) with the options –metagenomic (better ORF prediction for highly fragmented metagenomic sequences) and translation table 11. All ORFs were searched for similarities to the NCBI RefSeq Protein Database, using a standalone version of BlastP (Altschul et al., 1990) with the options for best top hit with an e-value $1x10^{-6}$.

3.7. Data management

The Rapid Annotations using Subsystems Technology (RAST) pipeline, is an automatic annotation server for microbial genomes designed for processing both raw sequence-reads datasets and already assembled contigs (Aziz et al., 2008). RAST has been built upon the framework provided by the SEED system (Overbeek et al., 2014) and constitutes four main tasks for metagenomic analysis: (1) Data normalization, (2) Using public databases for screening the sequences and for detecting the potential coding sequences, (3) Assessment of the results for functional gene annotation and taxonomic assignments, (4) Using the integrated SEED Viewer for result visualization.

The SEED continually integrates annotations from a wide variety of sources such as NCBI conserved domain database (CDD), the KEGG Enzyme database, Swiss-Prot, IMG, data from metabolic modeling, expression data, and literature references verifying annotations to analyze different microbial genomes and selected bins from metagenomic data. It offers an online service for genome annotation and comparison. Each user can register and upload datasets for further annotation.

The subsystems in seed are continuously subjected to quality control and the new subsystems are added to existing subsystems to cover previously un-annotated regions of the genomes. These strategies improve annotations in the SEED and their propagation via FIGfams into RAST. The genomes that annotated by RAST are then introduced into the SEED for further curation by SEED. In the other word, the SEED-based annotations comprises the cycle of SEED => FIGfam => RAST => SEED.

3.8. Phylogenetic construction of linked AprBA, 16S rRNA and McrA sequences

A phylogenetic tree was constructed from 107 full-length sequences (Appendix III) of linked A and B subunits of the adenosine 5′-phosphosulfate (APS)-reductase (AprBA) that are previously published (Stokke et al., 2012), in addition to the environmental AprBA sequences from the current Nyegga sediment metagenome (contig 00001). The combined dataset was submitted to the online PhyML program (http://phylogeny.lirmm.fr/) (Dereeper et al., 2008) for phylogenetic estimation. The multiple alignment of the sequences was performed using MUSCLE (Edgar, 2004), and Gblocks (Castresana, 2000) mode was selected for alignment curation. A maximum likelihood tree was constructed using the WAG amino acid substitution model matric. Bootstrap values were obtained from 100 replicates. Ribosomal RNA sequences, 16S rRNA, from the *Methanosarcinaceae* bin (contig01666) in addition to the 123 16S rRNA sequences (Appendix IV.) from different archaeal families were submitted to the online PhyML program (Dereeper et al., 2008) for phylogenetic tree construction. The processing steps and softwares used for tree construction were similar to the AprAB tree. The McrA genes (Appendix II.) were also recruited for phylogenetic tree construction. Same processing steps and softwares were applied for 36 sequences to conduct the phylogenetic construction. Stability of the trees was tested by changing the parameters.

For phylogenetic tree based on the 16S rRNA,the Newick file of the generated tree was submitted to the iTOL (Letunic and Bork, 2011) (http://itol.embl.de/) to edit and display the tree. The Newick files of the AprBA and McrA phylogenetic tree were submitted to the MEGA4(Tamura et al., 2007) for further edition and visualization.

4. Results and Discussion

4.1. Metagenome and taxonomic binning

The extracted DNA of Nyegga cold seep sediment (22cmbsf) was subjected to 454-pyrosequencing. Initially, 1001981 sequence reads with an average read length of 342 bp and average sequencing depth of 7.8x were generated and resulted in a 142.8 MB assembly; with a total of 22706 contigs and 10979 contigs > 500 bp with average size of 1362 (Table 4.1).

Table 4.1. Summary of Newbler v2.5.3 assembly.

Feature	***Value***
Number of reads	1001981
Number of assembled reads	420688
Number of Partial	79558
Number of Singletons	462969
Number of Repeats	729
Number of Outliners	25827
Number Too Short	12210
Number of assembled bases	18078455
Number of Contigs >500bp	10979
Total number of Contigs	22706
Largest Contig size	35034
Average Contig size	1362
N50 Contig size	1660

The binning was performed using Metawatt binner (Strous et al., 2012b) and a taxonomic profile was calculated for each bin. The contigs were binned into four bins with different qualities (Figure 12.). Only two of the four bins, bin I and II, had acceptable distinct taxonomic signature as well as a distinct sequencing coverage. The largest bin (bin I), with a GC content of 41.99% and assembly coverage of 12.09x contained 1545 contigs affiliated to the *Desulfobacteraceae* or in general *Deltaproteobacteria.* The genes designated to *Archaea*, *Methanosarcinaceae* were grouped into the bin II with the GC content of 49.79% and assembly coverage of 10.50x. Notably, both bins I and II contained contigs of other population of microorganisms, but the dominant species were clearly of *Desulfobacteraceae* and *Methanosarcinaceae*, respectively. Bin II harbored merely *Archaea*. The summary of the four bins is represented in Table 4.2. Bin III and IV, were examples of unsuccessful binning. Both bins, III and IV consisted of a mixture of contigs from different population which are distantly related e.g. in bin IV the contigs form *Desulfobacteraceae* population got mixed with the contigs from *Methanosarcinaceae* population. JS-1 and Candidate division OP9 bacterium family were categorized in the bin III with 730 contigs (Figure 12).

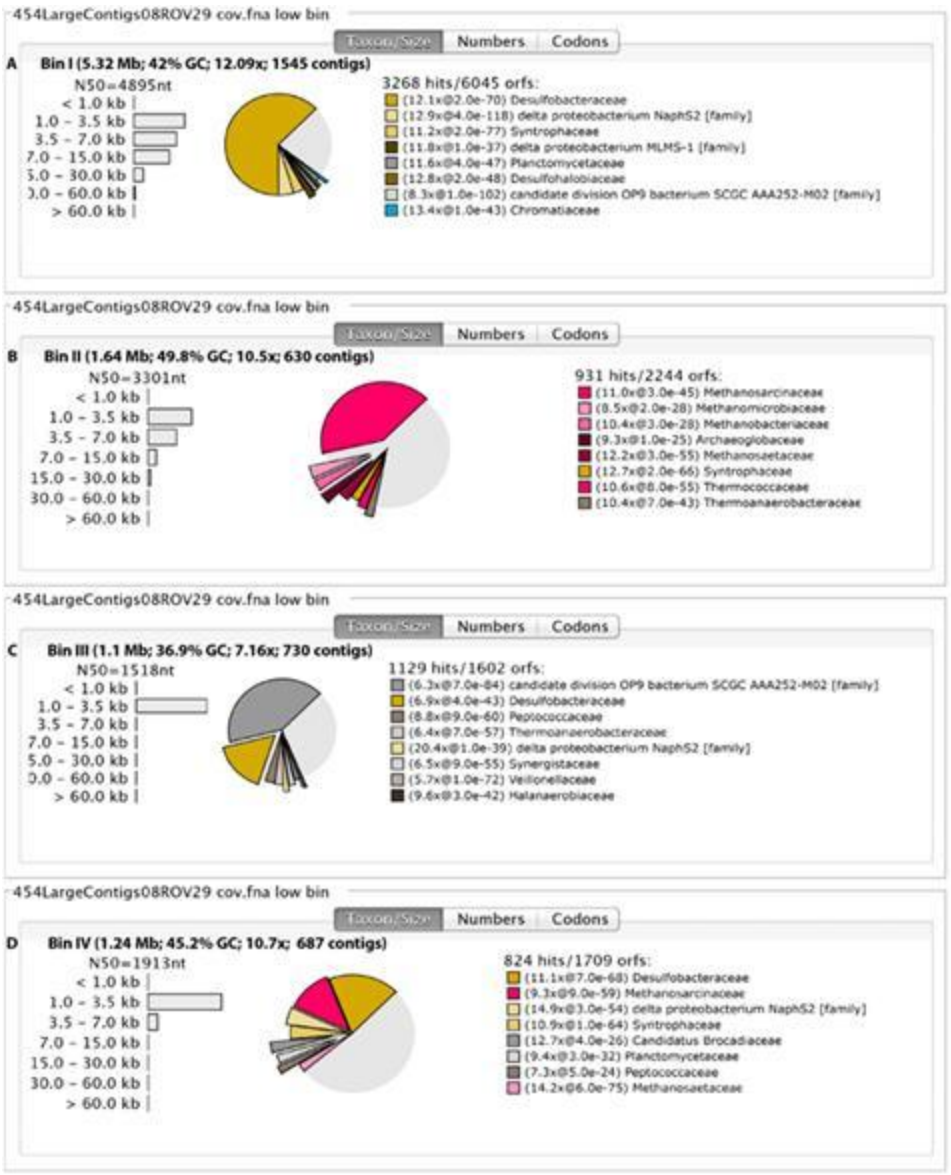

Figure 12. The figure shows an exploded pie chart of the taxonomic distribution of the extracted Metawatt bins I-IV (A-D). As inferred from the software, the distance of each pie slice from the center, is a measure for the median e-value of the associated hits, hence the larger the e-value the larger the distance from the center. Metawatt binner indicated that the dominant population in bin I and II are *Desulfobacteraceae* and *Methanosarcinaceae* respectively.

In order to further the taxonomic classification of bin I and II, respectively, genes encoding the evolutionary markers, AprBA and, 16S rRNA and McrA were extracted from the metagenomic bins after their annotation in RAST. The phylogenetic trees based on these genes were constructed to uncover what microbes are in our metagenomic sample and where those strains fit into the phylogenetic tree of life. The McrA and archaeal 16S rRNA, and AprBA genes were correctly clustered in the II and I bins, respectively.

Table 4.2. The summary of the Metawatt binner version 3.2, binning.

Bin	I	II	III	IV
Contigs	1545	630	730	687
Bin size (Mb)	5.32	1.64	1.10	1.24
N50 contig length (nt)	4895	3301	1518	1913
Percent GC %	41.99	49.79	36.88	45.17
Assembly coverage, x (sequencing depth)	12.09	10.50	7.16	10.70

Analysis of the rRNA gene content of the metagenome showed the presence of rRNA genes in 10 contigs. The 16S rRNA genes in contigs 00573 and 00658 showed high sequence identity to uncultured bacterium (AM229195.1 and JQ925104.1 respectively) and they were grouped into the third bin, which contained the mixture of *Desulfobacteraceae* and *Methanosarcinaceae*, whereas the 16S rRNA genes in contigs 02011 and 02868 were categorized in none of the bins uploaded into RAST. The 16S rRNA gene in contig01666 showed 99% percent of nucleotide identity to an uncultured archaeon 16S rRNA gene (clone fos0626f1; AJ890142) of ANME-2c (Meyerdierks et al., 2005). A simple phylogenetic analysis revealed that this 16S rRNA gene was affiliated with ANME-2c sequences (Appendix I).

A complete MCR operon (Figure 13.) was present in the bin II and the order of the genes encoding the subunits of the MCR complex was similar to a previous report of the gene organization of this complex in ANME-2c (Figure 2.)(Hallam et al., 2003).

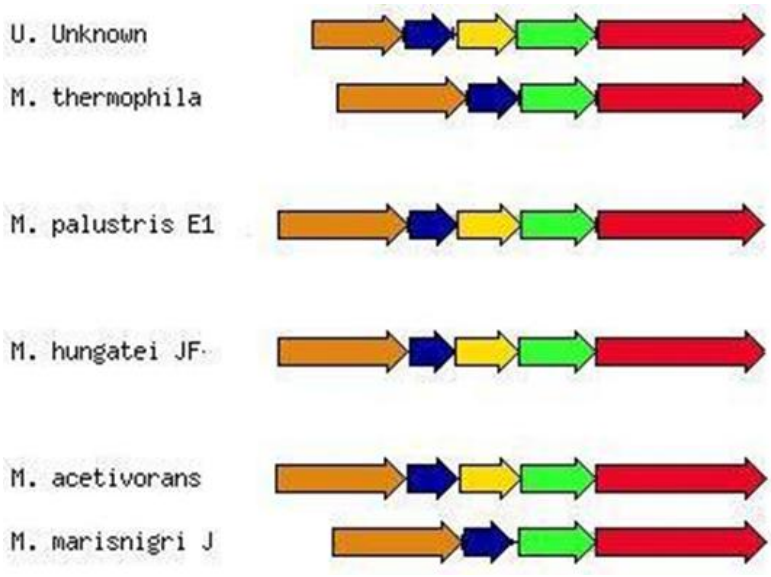

Figure 13. The Methyl coenzyme M reductase operon presented in contig00332 and comparison of gene organization in this operon with other microorganisms. Orange: Methyl-coenzyme M reductase subunit B, Blue: Methyl-coenzyme M reductase subunit D, Yellow: Methyl-coenzyme M reductase subunit C, Green: Methyl-coenzyme M reductase gamma subunit, Red: Methyl-coenzyme M reductase subunit alpha. The sequence presented in contig 00332 was labeled as unknown. The other organisms belong to the methanogens, in the order of *Methanomicrobiales*.

The unique McrA sequence presented in bin II (contig 00332) showed 91% sequence identity to the McrA sequence from ANME-2c (GZfos26B2; AAU83007.1). The phylogenetic analysis

further revealed that this sequence clustered with McrA from ANME-2c (GZfos26B2 and GZfos35D7) (Figure 14.).

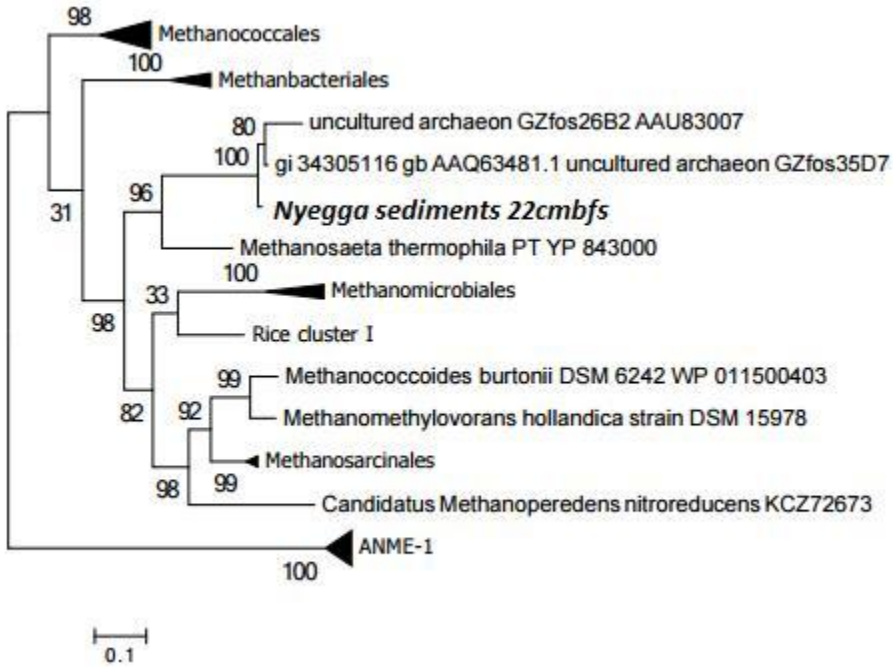

Figure 14. Phylogenetic tree of McrA sequences, including McrA on contig00332 from the Nyegga sediment at 20-22 cmbfs horizon. The tree is based on a MUSCLE alignment and constructed with the PhyML program using 100 bootstrap values.

Altogether, these results are in line with that 60% of the microbial community at this horizon in the Nyegga cold seep is dominated by ANME-2c (Roalkvam et al., 2011). Metawatt employs both compositional and homology approaches in order to cluster the contigs that arise from the same population (Strous et al., 2012b). In the taxonomic classification used in this study the database of reference genome sequences downloaded from NCBI (http://www.ncbi.nlm.nih.gov/) did not included sequences of ANME-2. This may explain why the Metawatt-analysis classified the contigs that presented in bin II, as *Methanosarcinaceae* rather than of ANME. ANME-2c is closely related to the *Methanosarcinales* (Knittel et al., 2005). In conclusion, the obtained results suggested that metagenome bin II represents ANME-2c.

The full length genes of AprBA from bin I indicated 86% sequence identity with *Desulfosarcina sp.* (WP_027353074.1) in the family of *Desulfobacteraceae*. This AprBA sequence clustered with AprBA sequences originating from a microbial mat collected from the Black Sea (Figure 15.) (Basen et al., 2011). A high AOM rate was reported for this microbial mat and the clustering of the Apr sequences with the *Desulforsarcina-Desulfococcus* group indicated that they originated from the bacterial partner in the methane-oxidizing consortium. The phylogenetic analysis of the AprBA sequences from Nyegga (22 cmbsf) thus suggested that bin I represented the bacterial partner of ANME-2c.

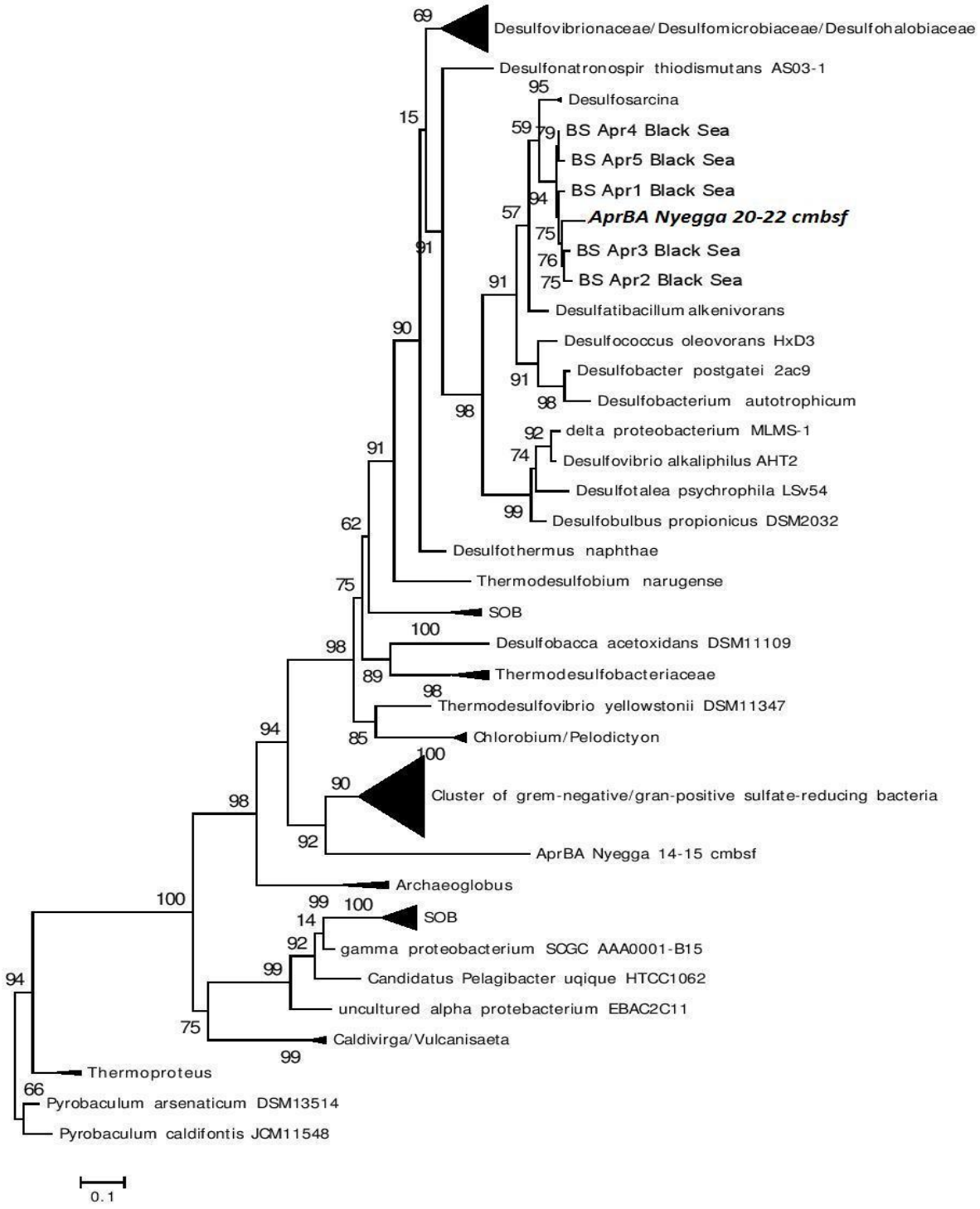

Figure 15. The phylogenetic tree of AprBA sequences, including AprBA on contig00001 from the Nyegga sediment from 22 cmbsf. The tree is based on a MUSCLE alignment and constructed with the PhyML program using 100 bootstrap values.

4.2. Annotation of metagenomic bins in RAST

The bin I, II and IV were uploaded into RAST for annotation. Due to the poor quality of the bin III and since the focus of this study is the investigation of AOM coupled with sulfate reduction, this bin was disregarded and was not uploaded into RAST for further analysis.

RAST uses public databases for screening the sequences and for detecting the potential coding sequences and tries to assign function to all genes in the genome. It performs this by grouping functions into operational subsystems and searching for the proteins that perform discrete functional roles. A subsystem is a collection of any number of proteins that are related in some functional or structural way and together implement a specific biological process or structural complex such as metabolic, signaling and regulatory pathway or structural complex. The summary of the three uploaded bins into RAST is presented in Table 4.3. In the largest bin which belongs to the *Desulfobacteraceae*, only 34% of the protein-encoding genes were covered by subsystems i.e. could be designated as protein encoding genes (PEGs) that are present in at least one subsystem. This indicates that difficulties of gene annotation in fragmented metagenomic samples such as from the Nyegga sediments.

Table 4.3. An overview of the three bins uploaded into RAST.

Bin	I*		II *		IV	
Domain	Bacteria		Archaea		Bacteria	
Size	5,321,697 bp		1,635,327 bp		1,235,088 bp	
Number of Contigs (with PEGs)	1545		630		687	
Number of Subsystems	329		82		50	
In subsystem	34%		13%		10%	
	Non-hypothetical	1855	Non-hypothetical	239	Non-hypothetical	134
	hypothetical	76	hypothetical	2	hypothetical	974
Out of subsystem	66%		87%		90%	
	Non-hypothetical	1167	Non-hypothetical	473	Non-hypothetical	352
	hypothetical	2741	hypothetical	1186	hypothetical	974
Number of Coding Sequences	5839		1900		1463	
Number of RNAs	57		18		14	

*Based on the phylogenetic analysis, the bin I, II can be named as *Desulfobacteraceae* and ANME-2c, respectively.

4.3. Anaerobic oxidation of methane (AOM)

In the ANME-2c bin, bin II, all genes encoding the enzymes involved in the seven steps of the methanogenic pathway were identified (Table 4.4.). Subunits of the enzymes involving in the methanogenesis pathway were annotated by RAST except the Coenzyme F_{420}- dependent N_5N_{10}-methylene tetrahydromethanopterin reductase (Mer) and Methylenetetrahydromethanopterin dehydrogenase (Mtd). The presence of a *mer* gene fragment, with the possible ANME-2c origin, was reported at the horizon (14–16 cmbsf) above our sample (Stokke et al., 2012). This result increased the possibility of finding these genes in our dataset although they were not annotated by RAST. The nucleotide sequence of *mer* was kindly provided by Dr.Stokke and was used as query sequence to find the possible similar sequence in our dataset using blast (http://blast.ncbi.nlm.nih.gov). Contigs 02138 and 05889 were found to harbor a putative *mer* gene. These sequences were subjected to the blastx and the presence of *mer* was confirmed. The one, which is called *mer1*, was located adjacent to a TATA-box binding protein gene in contigs 02138 (Figure 16A.) whereas contig 05889 contained only *mer* gene, designated *mer2*. Although contig 02138 was grouped in ANME-2c bin, RAST annotated only the TATA-box binding protein gene (Figure 16B.). Contig 05889 was not clustered in ANME-2c bin.

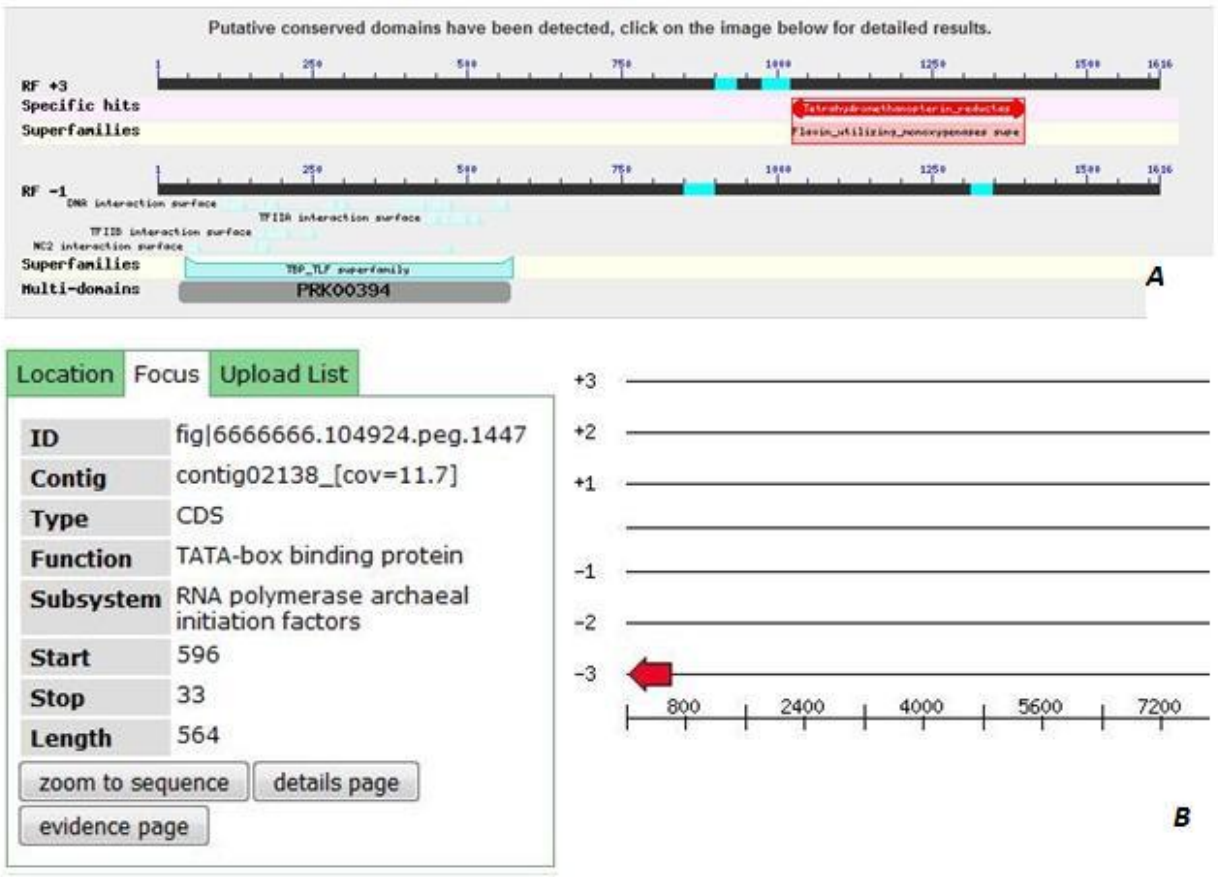

Figure 16. Panel (A); the blastx result of the sequence of contig 02138. The *mer* gene (red) was shown adjacent to the TATA box binding protein gene (blue). Panel (B); visualization of the same contig by RAST. Only TATA box binding protein was indicated by RAST.

Using the ORF finder (http://www.ncbi.nlm.nih.gov/gorf/orfig.cgi), provided by NCBI, two open reading frames were revealed that have the potential to encode the polypeptides with 187 and 281 amino acids respectively. These sequences were applied to the blastp and the same results were obtained. The longer polypeptide belonged to Mer and the other one to the TATA box binding protein. The contig 05889, which was shorter than the 02138, contained an ORF which encoded a *mer* polypeptide with 225 amino acids (data not shown). The *mer* sequences in contig 02138 and 05889 had respectively, 70% and 66% percent of nucleotide identity to *mer* from the known methanotroph *Candidatus Methanoperedens nitroreducens* (WP_048091521.1). Among the blastx top hits, the first one with high percent of nucleotide identity, 74%, belong to *Methanococcoides burtonii* (WP_011500359.1) within the order of *Methanosarcinales.*

Two sequences encoding methylenetetrahydromethanopterin dehydrogenase (*mtd)* were found in contigs 03373 and 08730 in blastx which were not annotated in RAST. According to the blastx result for *mtd* gene, both fragments of this gene were similar to members of *Methanosarcinales* with 72% and 74% of nucleotide identity, respectively. This percentage of identity to *Methanosarcinales* may be due to the lack of ANME-2c homolog sequences in public databases. Considering this and that ANME-2c related to the methanosarcina, the *mer* and *mtd* gene are likely to belong to the ANME-2c rather than the *Methanosarcinales.*

Altogether, these results identified the presence of a complete methanogenesis pathway in ANME-2c bin, bin II, suggested a potential for the ANME-2c population at 20-22cmbsf horizon of Nyegga sediments, to perform oxidation of methane via reverse methanogensis from CH_4 to CO_2. Previously, it has been demonstrated that ANME-2a/b and ANME-2d (Haroon et al., 2013a, Wang et al., 2014) have a complete reverse methanogenesis pathway, whereas ANME-1 lacks *mer* gene (Stokke et al., 2012). Our results supported that all ANME-2 subgroups i.e. ANME-2a/b, ANME-2c, ANME-d possess all the required genes for a complete methane-oxidizing pathway and are thus different from ANME-1 in this regard.

A survey of bin II did not support the possibility of the occurrence of the other proposed mechanisms of AOM i.e. reduction of nitrate/ nitrite or metal ions coupled to AOM, as no key enzymes involved in these processes were found. Since the nitrate/ nitrite reduction dependent to AOM has been reported only in fresh water so far (Cui et al., 2015), the absence of the genes involved in this process was expected.

Table 4.4. Identification of methanogenesis-associated genes in the sediment from 22cmbfs of Nyegga cold seeps.

Step	*Gene name*	*Abbreviation*	*Contig No.*	*RAST*
1	*Methyl-coenzyme M reductase subunit A*	*mcrA*	*00332*	*fig|6666666.104924.peg.441*
	Subunit B	*mcrB*	*00332*	*fig|6666666.104924.peg.437*
	Subunit C	*mcrC*	*00332*	*fig|6666666.104924.peg.439*
	Subunit D	*mcrD*	*00332*	*fig|6666666.104924.peg.438*
	Subunit G	*mcrG*	*00332*	*fig|6666666.104924.peg.440*
2	*Tetrahydromethanopetrin : coenzyme M methyltransferase subunit A*	*mtrA*	*00377*	*fig|6666666.104924.peg.506*
	Subunit B	*mtrB*	*00377*	*fig|6666666.104924.peg.507*
	Subunit C	*mtrC*	*00377*	*fig|6666666.104924.peg.508*
	Subunit D	*mtrD*	*00377*	*fig|6666666.104924.peg.509*
	Subunit E	*mtrE*	*00377*	*Not annotated*
	Subunit F	*mtrF*	*00377*	*fig|6666666.104924.peg.505*
	Subunit G	*mtrG*	*00377*	*fig|6666666.104924.peg.504*
	Subunit H	*mtrH*	*00377*	*fig|6666666.104924.peg.503*
3	*Coenzyme F_{420}- dependent N5N10-methylene tetrahydromethanopterin reductase*	*mer1* *mer2*	*02138* *05889**	*Not annotated*
4	*Methylenetetrahydromethanopterin dehydrogenase*	*mtd1*	*03373**	*Not annotated*
		mtd2	*08730**	
5	*N(5),N(10)-Methenyltetrahydromethanopterin cyclohydrolase*	*mch*	*01532*	*fig|6666666.104924.peg.1295*
			02264	*fig|6666666.104924.peg.1486*
			03490	*fig|6666666.104924.peg.1755*
6	*Formylmethanofuran - tetrahydromethanopterin N-formyltransferase*	*ftr*	*01632*	*fig|6666666.104924.peg.1320*
7	*Formylmethanofuran dehydrogenase subunit A*	*fmdA*	*00221*	*fig|6666666.104924.peg.273*
	Subunit B	*fmdB*	*00378*	*fig|6666666.104924.peg.514*
			03331	*fig|6666666.104924.peg.1716*
	Subunit C	*fmdC*	*00221*	*fig|6666666.104924.peg.274*
	Subunit D	*fmdD*	*00221*	*fig|6666666.104924.peg.274*
	Subunit E	*fmdE*	*00221*	*fig|6666666.104924.peg.271*
	Subunit F	*fmdF*	*00221*	*fig|6666666.104924.peg.272*
	Subunit G	*Not found*	-	-
	Subunit H	*Not found*	-	-

* Contig not found in ANME-2c bin.

4.4. Sulfur metabolism

RAST and blastx annotated all of the genes encoding enzymes required for the dissimilatory sulfate reduction pathway (Figure 5.) in the Nyegga metagenome from 22cmbsf (Table 4.5.). All enzymes were found in the *Desulfobacteriaceae* bin, bin I, and there were no similar sequences in the ANME-2c bin.

Since both AprAB and DsrAB enzymes are soluble, they require a membrane-linked electron transporter partner. QmoABC and DsrMKJOP complexes transfer electrons from membrane to AprAB and DsrAB respectively (Figure 17.). The *qmo* genes are conserved in all sulfate-reducing organisms and often found co-located with the *aprAB* genes (Grein et al., 2013). In the Nyegga metagenome, the genes encoding the AprBA and Sat were present in the largest contig, contig00001 in *Desulfobacteriaceae* bin, and are located adjacent to the genes encoding the QmoABC complex. The conserved gene organization of these genes in contig00001 from Nyegga sample and in other *Desulfobacteriaceae* is shown in Figure 18.

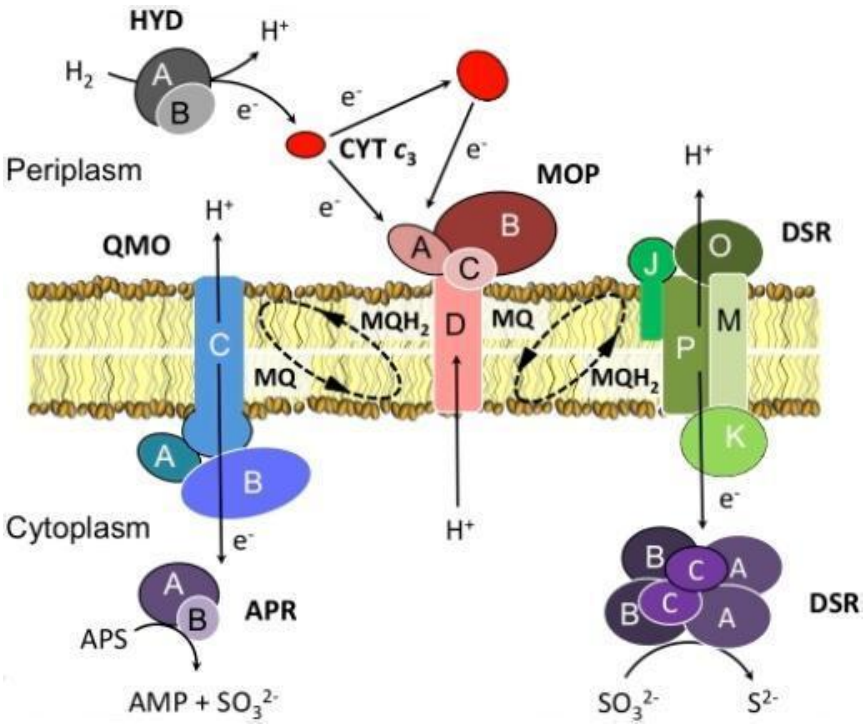

Figure 17. Schematic organization of the electron transfer chain. H2 is electron donor and sulfate is electron acceptor. Qmo and MKJOP complexes relay electrons from periplasm to the cytoplasmic enzymes APR and DSR respectively. APR catalyzes the reduction of Sulfate to sulfite and DSR reduces the sulfite to sulfide. Abbreviations: APS, adenosine-5'-phosphosulfate; AMP, adenosine monophosphate; MQ, menaquinone; MQH2, dihydromenaquinone. Adopted from (Spring et al., 2010).

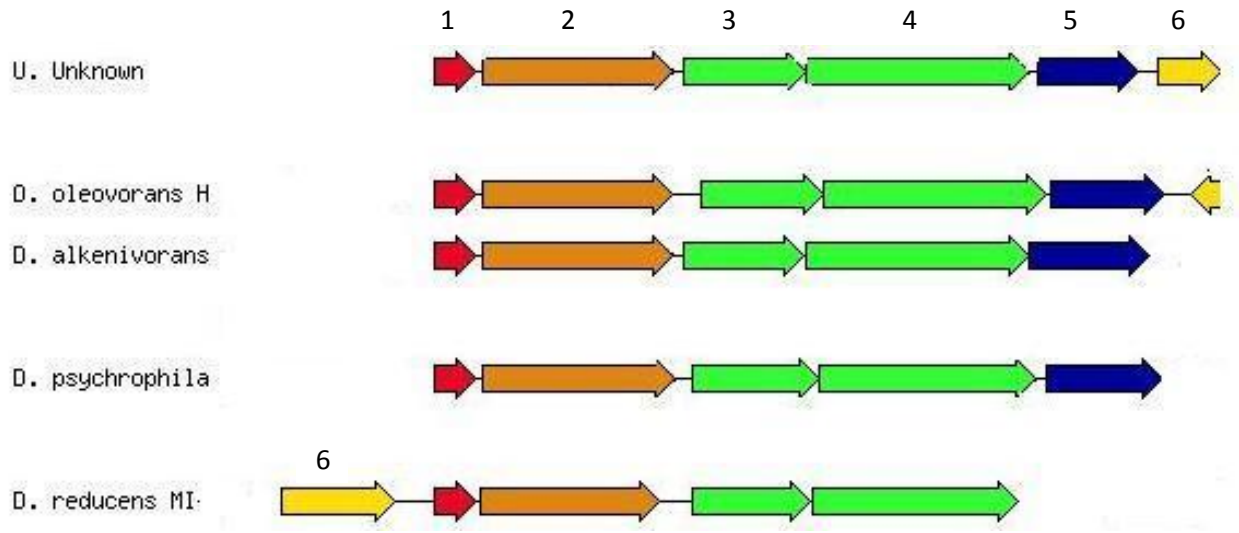

Figure 18. The gene organization of the AprAB, QmoABC and sat genes in different *Desulfobacteraceae*. 1-Red: Adenylylsulfate reductase beta-subunit (AprB), 2-Brown: Adenylylsulfate reductase alpha-subunit (AprA), 3-Green: CoB--CoM heterodisulfide reductase subunit A (QmoA), 4-Green: Heterodisulfide A/methylviologen-reducing hydrogenase,subunit delta (QmoB), 5: Heterodisulfide reductase, subunit E, putative (QmoC) and 6-yellow: Sulfate adenylyltransferase (Sat). The unknown organism is *Desulfobacteraceae* which is present in 22cmbfs of Nyegga region. All these genes are present in contig00001, which is the largest contig in our dataset. All the other organisms presented in this figure are the member of *Desulfobacteraceae*.

DsrMKJOP is a multimeric transmembrane complex that is encoded by the *dsrMKJOP* genes. In several organisms it has been observed that the *dsrMKJOP* genes cluster is associated with *dsrAB* cluster (Grein et al., 2013).The genes encoding the membrane-linked proteins, DsrMKJOP complex (Figure 19.) were annotated by RAST and present in contigs 00334 and 00402 in the *Desulfobacteraceae* bin. In contrast to the AprBA operon, the genes encoding Dsr complex (contig00237) (Appendix V.) were not co-localized with the genes coding the DsrMKJOP complex (contig00334 and 00402). This might be due to the fragmentation of environmental samples, which occurs during the sample processing. Previous metagenomic and metaproteomic analyses of ANME dominated communities have only identified the presence of key enzymes of dissimilatory sulfate reduction pathway.

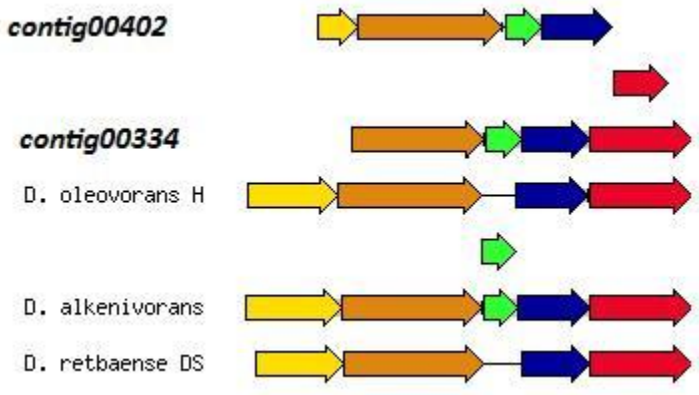

Figure 19. The gene organization of Sulfite reduction-associated complex DsrMKJOP in contig00402 and 00334 and three members of .*Desulfobacteraceae*. Yellow:DsrM, Borwon:DsrK, Green: DsrJ, Blue: Dsr:O, Red:DsrP

Table 4.5. Identification of genes encoding enzymes of dissimilatory sulfate reduction pathway in the sediment from 22cmbfs of Nyegga cold seeps.

Genes	*Abbreviation*	*Contig No.*	*RAST*
Sulfate Reduction			
Sulfate adenylyltransferase	*sat*	*00001*	*fig|6666666.104923.peg.28*
Adenylylsulfate reductase, subunit B	*aprB*	*00001*	*fig|6666666.104923.peg.23*
		02414	*fig|6666666.104923.peg.5184*
Adenylylsulfate reductase, subunit A	*aprA*	*00001*	*fig|6666666.104923.peg.24*
Sulfite Reduction			
Dissimilatory sulfite reductase, subunit alpha	*dsrA*	*00237*	*fig|6666666.104923.peg.2198*
		01209	*fig|6666666.104923.peg.4383*
Dissimilatory sulfite reductase, subunit beta	*dsrB*	*00237*	*fig|6666666.104923.peg.2197*
		00339	*fig|6666666.104923.peg.2636*
Dissimilatory sulfite reductase, subunit gamma	*dsrD*	*00090*	*fig|6666666.104923.peg.1165*
		00303	*fig|6666666.104923.peg.2457*
		03728	*fig|6666666.104923.peg.5710*
Membrane-bound electron transfer to terminal acceptor			
Heterodisulfide reductase, subunit E, putative	*qmoC*	*00001*	*fig|6666666.104923.peg.27*
		00082	*fig|6666666.104923.peg.1115*
		00223	*fig|6666666.104923.peg.2089*
Heterodisulfide reductase, subunit A/methylviologen-reducing hydrogenase,subunit delta	*QmoB*	*00001*	*fig|6666666.104923.peg.26*
		00082	*fig|6666666.104923.peg.1117*
		00138	*fig|6666666.104923.peg.1575*
		00138	*fig|6666666.104923.peg.1576*
		00223	*fig|6666666.104923.peg.2090*
		00223	*fig|6666666.104923.peg.2091*
		00444	*fig|6666666.104923.peg.3054*
		00463	*fig|6666666.104923.peg.3134*
		00736	*fig|6666666.104923.peg.3751*
		00779	*fig|6666666.104923.peg.3836*
		01111	*fig|6666666.104923.peg.4305*
		02396	*fig|6666666.104923.peg.5177*
		03445	*fig|6666666.104923.peg.5628*
CoB--CoM heterodisulfide reductase subunit A	*QmoA*	*00001*	*fig|6666666.104923.peg.25*
Sulfite reduction-associated complex DsrMKJOP multiheme protein DsrJ	*DsrJ*	*00334*	*fig|6666666.104923.peg.2610*
		00402	*fig|6666666.104923.peg.2878*
Sulfite reduction-associated complex DsrMKJOP iron-sulfur protein DsrO (=HmeA)	*DsrO*	*00334*	*fig|6666666.104923.peg.2609*
		00402	*fig|6666666.104923.peg.2877*

Sulfite reduction-associated complex DsrMKJOP protein DsrM (= HmeC)	*DsrM*	*00334* *00402*	*fig|6666666.104923.peg.2880* *fig|6666666.104923.peg.2881* *fig|6666666.104923.peg.5046*
Sulfite reduction-associated complex DsrMKJOP protein DsrK (=HmeD)	*DsrK*	*00334* *00402*	*fig|6666666.104923.peg.2611* *fig|6666666.104923.peg.2879* *fig|6666666.104923.peg.2946*
Sulfite reduction-associated complex DsrMKJOP protein DsrP (= HmeB)	*DsrP*	*00334* *00402*	*fig|6666666.104923.peg.2608* *fig|6666666.104923.peg.2876*

It has been proposed that the hydrogen cycling leads to energy conservation in sulfate respiration (Keller and Wall, 2011, Ramos et al., 2012) (Figure 6.). In this study, neither hydrogenases nor lactate dehydrogenases were identified; therefore, hydrogen cycling as an energy conservation mechanism seems unlikely. Altogether, our dataset could not address the mechanisms behind energy conservation in *Desulfobacteraceae*.

4.4.1. Implications for models of AOM

The metagenomic analysis of the Nyegga sediments has revealed genes encoding all reactions in the major metabolic pathway needed for AOM with sulfate. However, the data have not clarified which of the two putative key-players, ANME-2c or the *Desulfobacteriaceae* that perform sulfate reduction. According to the recent model proposed by Milucka (Milucka et al., 2012), ANME performs reduction of sulfate to zero-valent sulfur compounds (S^0) through a non-canonical pathway for dissimilatory sulfate reduction. The formed S^0 is then taken up by the *Deltaproteobacteria* and is reduced to sulfide through disproportionation to sulfide and sulfate (Milucka et al., 2012). Although genes encoding enzymes of the canonical dissimilatory sulfate reduction pathway were found in the *Desulfobacteraceae* bin, they may catalyze disproportionation rather than dissimilatory sulfate-reduction. More studies are needed to clarify this. It has been shown that bacterial partner of ANME-2 and -3 are mostly from *Desulfobulbaceae* (Pernthaler et al., 2008), which capable of disproportionation using the known enzymes Sat, AprAB and Dsr (Lovley and Phillips, 1994). Enzymes involved in dissimilatory sulfate reduction pathway with the archaeal origins was not found, therefore the enzymatic mechanisms of sulfate reduction to S^0, by archaea, still remains unclear (Milucka et al., 2012). In the current metagenomic dataset, the genes of enzymes involved in canonical dissimilatory sulfate reduction pathway were found in the *Desulfobacteraceae* bin, but due to the lack of geochemical information about the rate of the sulfate reduction: AOM at this site, it was not possible to support this hypothesis nor designated their role in disproportionation rather than canonical dissimilatory sulfate reduction pathway.

The spherical shell-type or mixed type consortia of ANME-2c with sulfate reducing bacteria (SRB) was also reported (Milucka et al., 2012, Orphan et al., 2002, Knittel et al., 2005) and reinforced the hypothesis that, in AOM consortia, anaerobic oxidation of methane is mediated by ANME-2 and sulfate reduction is catalyzed by the ANME-associated SRB (Wegener et al., 2008,

Basen et al., 2011). Our metagenomic study indicated the presence of consortia in the selected sample. The similarity of the deduced Sat, AprA, AprB, DsrAB sequences to the sequences from the known *Deltaproteobacteria* (*Desulfobacteraceae* at family level) with high present of identity fortified the probability that the bacterial partner in the methane-oxidizing consortium is a member of this group. The phylogenetic assessment based on the combined AprBA (Figure 15.) and 16srRNA (Stokke et al., 2012, Roalkvam et al., 2011) confirmed that *Desulfobacteraceae* constituted the dominant bacterial population at 22cmbfs of Nyegga cold seep sediment and proposed that this population might be associated bacterial partner of ANME-2c.

4.5. Carbon dioxide fixation

The carbon assimilation of many methanogens, and sulfate reducing bacteria (SRB) through the reductive acetyl-CoA has been reported (Berg et al., 2010, Hugler and Sievert, 2011). Kellermann and colleagues (Kellermann et al., 2012) have reported preferentially assimilation of inorganic carbon by both archaea and bacteria mediating AOM in hydrothermal sediments. It was demonstrated that the methanotrophic archaea, ANME-1, utilize methane as an energy source and not for carbon assimilation, and act as autotrophic methane oxidizers. However, the carbon assimilation was strongly accelerated in the presence of methane (Kellermann et al., 2012).

The acetyl-CoA pathway in methanogens involve mostly the same enzymes as in the methanogenesis (Figure 20.), however, the enzyme Carbon monoxide dehydrogenase/acetyl-CoA synthase is needed for catalyzing the formation of acetyl-CoA. Although methanogens and sulfate reducing bacteria share most of the steps in one-carbon metabolism, there are some differences (Figure 20.); the reduction of CO_2 to formate and activation of formate is performed by Formate dehydrogenase and 10-Formyl-H_4-folate synthetase using NADP in SRB, whereas this reaction is carried out by Formyl-methanofuran dehydrogenase and Formyl transferase using ferredoxin (Fuchs, 2011).

Genes that encode enzymes responsible for the steps in the acetyl-CoA pathway were identified in our metagenomic dataset (Table 4.6) and the presence of these enzymes, specifically the key enzyme CO dehydrogenase/acetyl-CoA synthase, found in the both bins designated for ANME-2c and *Desulfobacteraceae*, was in line with the previous reports and sugested CO_2 fixation through acetyl-CoA pathway by these microorganisms.

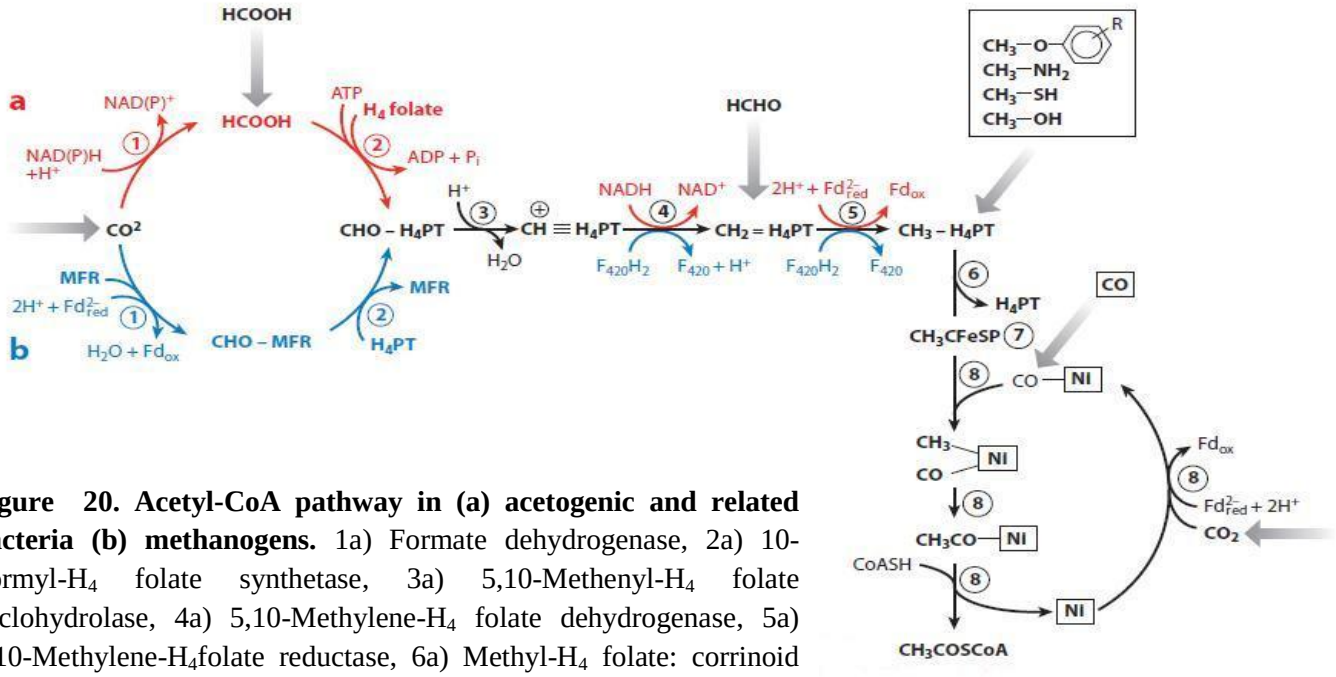

Figure 20. Acetyl-CoA pathway in (a) acetogenic and related bacteria (b) methanogens. 1a) Formate dehydrogenase, 2a) 10-Formyl-H_4 folate synthetase, 3a) 5,10-Methenyl-H_4 folate cyclohydrolase, 4a) 5,10-Methylene-H_4 folate dehydrogenase, 5a) 5,10-Methylene-H_4folate reductase, 6a) Methyl-H_4 folate: corrinoid iron-sulfur protein methyltransferase, 7a) Corrinoid iron-sulfur protein.1b) Formyl-methanofuran dehydrogenase, 2b) Formyl transferase, 3b) 5, 10-Methenyl-tetrahydromethanopterin, 4b) 5,10-Methylene-H_4-methanopterin dehydrogenase, 5b) 5,10-Methylene-H4-methanopterin reductase, 6b) Methyl-H_4-methanopterin: corrinoid iron-sulfur protein methyltransferase, 7b) Corrinoid iron-sulfur protein.8) CO dehydrogenase/acetyl-CoA synthase. The electron donors for each enzyme differ in bacteria and archaea. Adopted from (Fuchs, 2011).

The enzymes: Formyl-methanofuran dehydrogenase (Fd^{2-}red), 5,10-Methenyl-tetrahydromethanopterin (H_4 methanopterin) cyclohydrolase, 5,10-Methylene-H_4-methanopterin dehydrogenase ($F_{420}H_2$) and 5,10-Methylene-H_4-methanopterin reductase ($F_{420}H_2$*)* in ANME-2c bin are categorized in the one carbon metabolism in the subcategory of methanogenesis and are employed to reduce CO_2 to CH_3 (Table 4.4.). Therefore, only the key enzyme of this pathway from ANME-2c bin was presented in table 4.6. Since the bacterial enzymes involved in acetyl-CoA pathway differ from archaeal ones, the complete set of genes involved in this pathway from *Desulfobacteraceae* bin were analyzed and shown in table 4.6.

Table 4.6. Identification of genes involved in CO_2 fixation through acetyl-CoA pathway in ANME-2c and *Desulfobacteraceae* present in the sediment from 22cmbfs of Nyegga cold seeps.

	ANME-2C		
STEP	***GENES***	***Contig No.***	***RAST***
	CO dehydrogenase/acetyl-CoA synthase (Fd2−red)	*00319**	
		02467	
		04921	*Not annotated*
		05060	
		09051	
	Desulfobacteraceae		
	GENE	***Contig NO.***	***RAST***
1	*Formate dehydrogenase chain D*	*00316***	*fig|6666666.104923.peg.2524*
		*00334***	*fig|6666666.104923.peg.2607*
	Formate dehydrogenase O alpha subunit	*00241***	*fig|6666666.104923.peg.2209*
	Formate dehydrogenase-O, major subunit	*00155***	*fig|6666666.104923.peg.1667*
		*00534***	*fig|6666666.104923.peg.3327*
	NAD-dependent formate dehydrogenase alpha subunit	*00534***	*fig|6666666.104923.peg.3326*
		*02941***	*fig|6666666.104923.peg.5416*
		*04003***	*fig|6666666.104923.peg.5787*
2	*10-Formyl-H4folate synthetase (ADP forming)*	*Not Found*	-
3	*5,10-Methenyl-H4folate cyclohydrolase*	*Not Found*	-
4	*5,10-Methylene-H4folate dehydrogenase*	*Not Found*	-
5	*5,10-Methylene-H4folate reductase (Fd2− red)*	*00444***	*fig|6666666.104923.peg.3051*
		*00557***	*fig|6666666.104923.peg.3383*
6	*Methyl-H4folate:corrinoid iron-sulfur protein*	*Not Found*	
7	*Corrinoid iron-sulfur protein (CFeSP)*		
	Larg subunit	*00209***	*fig|6666666.104923.peg.1999*
	Small subunit	*00444***	*fig|6666666.104923.peg.3050*
8	*CO dehydrogenase/acetyl-CoA synthase (Fd2−red)*	*00209***	*fig|6666666.104923.peg.2001*
		06387	
		10568	

*Contigs found in ANME-2c bin / ** Contigs found in *Desulfobacteriacaea* bin

Another possible pathway for CO_2 fixation is the reductive citric acid cycle (Figure 9.). This cycle has been found in various groups of anaerobic *Deltaproteobacteria* (Figure 7.). It is reversal of the citric acid cycle and generates acetyl-CoA from CO_2 instead of oxidation of acetyl-CoA and production of energy. The genes encoding the Malate dehydrogenase, Fumarate hydratase, Isocitrate dehydrogenase and Aconitase were retrieved from *Desulfobacteraceae* bin, but the key enzyme ATP citrate lyase was absent (Table 4.7.).

Table 4.7. Identification of genes encoding the enzymes involved in reductive citric acid cycle in the sediment from 22cmbfs of Nyegga cold seeps. All the genes retrieved from *Desulfobacteraceae* bin.

Gene	*Contig No.*	*RAST*
Malate dehydrogenase	*02090*	*fig|6666666.104923.peg.5012*
Fumarate hydratase class I	*00546*	*fig|6666666.104923.peg.3353,*
	00751	*fig|6666666.104923.peg.3778*
	*03999**	
Isocitrate dehydrogenase	*00423*	*fig|6666666.104923.peg.2965,*
	03480	*fig|6666666.104923.peg.5642,*
	03480	*fig|6666666.104923.peg.5643*
Aconitate hydratase	*00211*	*fig|6666666.104923.peg.2016,*
	00274	*fig|6666666.104923.peg.2359,*
	01898	*fig|6666666.104923.peg.4878,*
	01898	*fig|6666666.104923.peg.4879,*
	01972	*fig|6666666.104923.peg.4933*

* Contig not found in *Desulfobacteraceae bin*

The occurrence of SRB and ANME in marine sediment at methane seeps has been reported, however, none of the microorganisms involved in methanotrophic consortia have not yet been isolated in pure culture, and our understanding about these SRBs, which are mainly relatives of *Desulfosarcina* or *Desulfobulbus,* and the range of electron donors is still incomplete. SRB may be organotrophic, using organic carbon compounds, such as lactate, formate, acetate, and pyruvate, or lithoautotrophic, and use hydrogen gas (H_2) as an electron donor. In another classification, SRB are grouped into two main groups: those that degrade organic compounds incompletely to acetate and those that degrade organic compounds completely to carbon dioxide. The latter group commonly also uses acetate as a growth substrate using either reductive citric acid cycle or acetyl-CoA pathway (Madigan et al., 2011).

The experimental evidence have refuted the electron shuttle in form of an organic compound such as formate, acetate, glucose, lactate (Meulepas et al., 2010, Moran et al., 2008). In accordance with those studies no formate dehydrogenase and no lactate dehydrogenase have been annotated using RAST and Blastx in *Desulfobacteraceae* bin.

According to our phylogenetic tree based on AprAB, SRB from *Desulfobacteraceae* family dominated at 22cmbfs of Nyegga sediments. It has been reported that CO_2 is the main carbon source of the SRB partner in AOM consortia and direct methane uptake or uptake of methane-derived organic intermediates is not significant in lipid biosynthesis in these microorganisms (Wegener et al., 2008). The presence of the gene encoding the key enzyme of the CO dehydrogenase/acetyl-CoA synthase (Fd2−red) fortifies the CO_2 fixation by *Desulfobacteraceae* using the acetyl-CoA pathway.

Dsulfosarcina (within the *Desulfobacteraceae* family) belongs to the group of SRB that degrade organic compounds completely to carbon dioxide and commonly also use acetate as a growth

substrate (Madigan et al., 2011). In this case, the enzymes of acetyl-CoA pathway might be used for acetate oxidation rather than CO_2 reduction. The enzymes phosphotransacetylase and acetyl kinase, which are involved in acetate oxidation, were retrieved in our data set using blastx. They were not annotated by RAST. However, blasting the sequences of these genes showed high sequence identity to other microorganisms belonging to neither SRBs nor ANME-2c. Since these fragments are so short, it is difficult to assign them to a specific bin. This suggested that the enzyme, CO dehydrogenase/acetyl-CoA synthase present in *Desulfobacteraceae*, catalyzes the acetyl-CoA pathway in reductive direction rather than oxidative. However, due to the lack of physio-chemical information, meta-transcriptomic data and lack of the FISH and isotopic tracer results, it is impossible to prove the presence of acetate in the environment and predict its consumption and/or generation by each of the microorganisms present in consortia.

Although the absence of ATP citrate lyase could diminish the probability of the recruiting the reductive citric acid cycle by *Desulfobacteraceae* to reduce CO_2 but it has been reported that some bacteria that might harbor the reductive citric acid cycle do not contain an obvious gene for ATP citrate lyase and instead use another type of this enzyme (Fuchs, 2011). On the other hand most of the annotated enzymes are also involved in the citric acid cycle are present, but their presence in the dataset does not indicate their involvement in reductive or oxidative direction. Given that some facultative, strict anaerobes reverse the cycle for the complete oxidation of acetyl-CoA, in the presence of a suitable organic substrate and an electron acceptor such as sulfate (Fuchs, 2011). Therefore, it is difficult to elucidate the employment of this cycle for CO_2 fixation.

4.6. Nitrogen fixation

The nitrogenase complex carries out the fixation of nitrogen by reducing molecular dinitrogen (N_2) to ammonium (NH^+_4). It consists of two protein complex; dinitrogenase and dinitrogenase reductase. In methanogens nitrogenase complex is encoded by a single operon consists of six genes. *nifH* encodes the homodimer of nitrogenase reductase, the α and β subunits of nitrogenase are encoded by *nifD* and *nifK* respectively, and *nifE* and *nifN* are required for iron-molybdenum cofactor (FeMoCo) synthesis (Leigh, 2000). Based on the RAST annotation, no genes were identified that could be involved in N_2-fixation. However, several fragments encoding the enzymes involved in the diazotrophy process were identified in Blastx file, belonging to the *Methanosarcina* (Table 4.8.). Due to the shortness of the sequences, only in contig 02484, *nifH* and *nifD* were co-located as tandem a sequences, which were consistent with the previous reports (Leigh, 2000). In addition, some sequences encoding proteins involved in iron-molybdenum cofactor biosynthesis were present, but not in a cluster. Although the *nifH* and *nifD* are present in our dataset, but the other requirements for the nitrogen fixation process are missed. It may be due to the highly fragmented dataset.

The diazotrophiy is distributed widely among the prokaryotes including bacteria and archaea. Several bacteria carry out nitrogen fixation, whereas the methanogens are the only cultivated

archaeal group that has been shown to perform this process. Recently, nitrogen fixation in ANME-2 has been suggested (Dekas et al., 2014). The occurrence of ANME-2 in the consortia with SRBs has been reported and it has been suggested that ANME-2 are the dominant diazotrophs in deep-sea methane seep sediment (Dekas et al., 2014). Consistent with this, several short fragments with high identity to the bacterial nif operon genes were found in our dataset (data not shown). However, all were categorized in the broad groups, either the uncultured microorganisms or D*eltaproteobacteria*. Overall, the presence of sequences involved in the nitrogen fixation suggested a potential for the ANME to take part in this process. The shortness and fragmentation of the sequences may lead to difficulties in binning and finally gene annotation. This could be the possible reason why RAST was not able to annotate the genes involved in nitrogen fixation. This also illustrates how challenging it is to perform a metagenomic analysis when the fragments are short and the additional information is missing.

Table 4.7. The list of the archaeal nif operon genes.

Gene	***Contig NO.***	***Length (bp)***
Dinitrogenase iron-molybdenum cofactor biosynthesis	00366	363
Dinitrogenase reductase, partial uncultured ,*NifH*	02484	246
Dinitrogenase alpha subunit	02484	318
Dinitrogenase reductase NifH, partial	03068	591
Dinitrogenase alpha subunit	03299	1032
Dinitrogenase reductase, partial	03432	420
Dinitrogenase iron-molybdenum cofactor biosynthesis	03478	297
Dinitrogenase iron-molybdenum cofactor biosynthesis protein	04675	345
Dinitrogenase reductase	10845	399

5. Conclusion

The culture-independent surveys of microbial assemblages within the methane-rich sediments from Nyegga have provided insight into microbial functions and population structure in this habitat. Combining phylogenetic information and analysis of the putative functional genes have provided a glimpse into specific microorganisms associated with the anaerobic oxidization of methane. Phylogenetic evidences obtained in this study strongly support the involvement of a syntrophic consortium, consisting of ANME-2c, and SRB belonging to the *Desulfosarcina–Desulfococcus* group, in AOM. A complete set of genes encoding enzymes involved in the reverse methanogenesis, dissimilatory sulfate reduction pathway and the electron transferring complexes, fortifies the mediation of methane oxidation coupled to sulfate reduction rather than

reduction of other electron acceptors. Although a complete set of genes involved in CO_2 fixation were not retrieved, the identification of the key enzyme, CO-dehydrogenase/acetyl-CoA synthase in the dataset assigned to both dominant populations in this site is in consistent with reports of close relatives (methanogens, *Desulfosarcina*) to fix inorganic carbon through acetyl-CoA pathway. The data obtained emphasize the importance of using multiple molecular approaches for the identification of major functional taxa in environmental samples and from a fundament for further more advanced meta-omics approaches involving meta-transcriptomic and meta-proteomics.

.

6. Future work

Although the metagenomic approach used in this study allowed identification of genes encoding the key enzymes involved in major metabolic pathways in sulfate-dependent AOM, the acetyl-CoA pathway and in nitrogen fixation in Nyegga cold seep sediments, there are still many missing parts to complete the whole picture of life in Nyegga methane seepage. First, some of the identified pathways were incomplete and some of the identified genes were short and incomplete. This also made it problematic to identify for example the organization of genes in operons or gene clusters. The metagenomic data set consisted of 1001981 sequence reads. By collecting a higher number of reads with other sequencing technologies rather than the 454-technology, used in this study, such as the Illumina technology, a higher number of reads could be achieved and more complete genome information could be obtained. This could also have improved the binning procedure.

This project is a metagenome-based analysis i.e. predicting the functional metabolic capacity of this site based on the non-cultural studies performed on DNA level. Given that the presence of a gene does not represent its expression, hence, a metagenomic analysis needs to be coupled to metatranscriptomic and metaproteomic studies to give the better view of what is ongoing at this site. In addition, in the case of enzymes which are shared between two or more metabolic pathways, even the presence of active protein is not representative of the specific pathway, unless the additional information about the geological and geochemical condition of the site of interest is available. For example the annotation of the genes encoding for AprAB and Dsr subunits does not help us to clarify whether these enzymes catalyze disproportionation or dissimilatory sulfate reduction. In addition, information about the reaction rates of methane oxidation and sulfate-reduction, if the stociometry is 1:1 or not, would help to understand if for instance the SRB could catalyze other processes in addition to taking part in AOM.

Moreover, FISH analyses are needed to evaluate if ANME-2c are associated to an SRB partner. Finally, culture-based experiments could facilitate other analyses for example isotopic tracer studies which could help to track different elements through biochemical reactions and their transfer among the organisms present in the culture.

7. References

ALTSCHUL, S. F., GISH, W., MILLER, W., MYERS, E. W. & LIPMAN, D. J. 1990. Basic local alignment search tool. *J Mol Biol,* 215**,** 403-10.

ALVARADO, A., MONTAÑEZ, L., PALACIO MOLINA, S. L., OROPEZA, R., LUEVANOS ESCARENO, M. P. & BALAGURUSAMY, N. 2014. Microbial trophic interactions and mcrA gene expression in monitoring of anaerobic digesters. *Frontiers in Microbiology,* 5.

ANDERSON, T. R. & RICE, T. 2006. Deserts on the sea floor: Edward Forbes and his azoic hypothesis for a lifeless deep ocean. *Endeavour,* 30**,** 131-7.

ANGIUOLI, S. V., MATALKA, M., GUSSMAN, A., GALENS, K., VANGALA, M., RILEY, D. R., ARZE, C., WHITE, J. R., WHITE, O. & FRICKE, W. F. 2011. CloVR: a virtual machine for automated and portable sequence analysis from the desktop using cloud computing. *BMC Bioinformatics,* 12**,** 356.

AOSHIMA, M. 2007. Novel enzyme reactions related to the tricarboxylic acid cycle: phylogenetic/functional implications and biotechnological applications. *Appl Microbiol Biotechnol,* 75**,** 249-55.

AZIZ, R. K., BARTELS, D., BEST, A. A., DEJONGH, M., DISZ, T., EDWARDS, R. A., FORMSMA, K., GERDES, S., GLASS, E. M., KUBAL, M., MEYER, F., OLSEN, G. J., OLSON, R., OSTERMAN, A. L., OVERBEEK, R. A., MCNEIL, L. K., PAARMANN, D., PACZIAN, T., PARRELLO, B., PUSCH, G. D., REICH, C., STEVENS, R., VASSIEVA, O., VONSTEIN, V., WILKE, A. & ZAGNITKO, O. 2008. The RAST Server: rapid annotations using subsystems technology. *BMC Genomics,* 9**,** 75.

BASEN, M., KRUGER, M., MILUCKA, J., KUEVER, J., KAHNT, J., GRUNDMANN, O., MEYERDIERKS, A., WIDDEL, F. & SHIMA, S. 2011. Bacterial enzymes for dissimilatory sulfate reduction in a marine microbial mat (Black Sea) mediating anaerobic oxidation of methane. *Environ Microbiol,* 13**,** 1370-9.

BEAL, E. J., HOUSE, C. H. & ORPHAN, V. J. 2009. Manganese- and iron-dependent marine methane oxidation. *Science,* 325**,** 184-7.

BENTLEY, D. R., BALASUBRAMANIAN, S., SWERDLOW, H. P., SMITH, G. P., MILTON, J., BROWN, C. G., HALL, K. P., EVERS, D. J., BARNES, C. L., BIGNELL, H. R., BOUTELL, J. M., BRYANT, J., CARTER, R. J., KEIRA CHEETHAM, R., COX, A. J., ELLIS, D. J., FLATBUSH, M. R., GORMLEY, N. A., HUMPHRAY, S. J., IRVING, L. J., KARBELASHVILI, M. S., KIRK, S. M., LI, H., LIU, X., MAISINGER, K. S., MURRAY, L. J., OBRADOVIC, B., OST, T., PARKINSON, M. L., PRATT, M. R., RASOLONJATOVO, I. M., REED, M. T., RIGATTI, R., RODIGHIERO, C., ROSS, M. T., SABOT, A., SANKAR, S. V., SCALLY, A., SCHROTH, G. P., SMITH, M. E., SMITH, V. P., SPIRIDOU, A., TORRANCE, P. E., TZONEV, S. S., VERMAAS, E. H., WALTER, K., WU, X., ZHANG, L., ALAM, M. D., ANASTASI, C., ANIEBO, I. C., BAILEY, D. M., BANCARZ, I. R., BANERJEE, S., BARBOUR, S. G., BAYBAYAN, P. A., BENOIT, V. A., BENSON, K. F., BEVIS, C., BLACK, P. J., BOODHUN, A., BRENNAN, J. S., BRIDGHAM, J. A., BROWN, R. C., BROWN, A. A., BUERMANN, D. H., BUNDU, A. A., BURROWS, J. C., CARTER, N. P., CASTILLO, N., CHIARA, E. C. M., CHANG, S., NEIL COOLEY, R., CRAKE, N. R., DADA, O. O., DIAKOUMAKOS, K. D., DOMINGUEZ-FERNANDEZ, B., EARNSHAW, D. J., EGBUJOR, U. C., ELMORE, D. W., ETCHIN, S. S., EWAN, M. R., FEDURCO, M., FRASER, L. J., FUENTES FAJARDO, K. V., SCOTT FUREY, W., GEORGE, D., GIETZEN, K. J., GODDARD, C. P., GOLDA, G. S., GRANIERI, P. A., GREEN, D. E., GUSTAFSON, D. L., HANSEN, N. F., HARNISH, K., HAUDENSCHILD, C. D., HEYER, N. I., HIMS, M. M., HO, J. T., HORGAN, A. M., et al. 2008. Accurate whole human genome sequencing using reversible terminator chemistry. *Nature,* 456**,** 53-9.

BERG, I. A., KOCKELKORN, D., RAMOS-VERA, W. H., SAY, R. F., ZARZYCKI, J., HUGLER, M., ALBER, B. E. & FUCHS, G. 2010. Autotrophic carbon fixation in archaea. *Nat Rev Microbiol,* 8**,** 447-60.

BOETIUS, A., RAVENSCHLAG, K., SCHUBERT, C. J., RICKERT, D., WIDDEL, F., GIESEKE, A., AMANN, R., JORGENSEN, B. B., WITTE, U. & PFANNKUCHE, O. 2000a. A marine microbial consortium apparently mediating anaerobic oxidation of methane. *Nature,* 407**,** 623-6.

BOETIUS, A., RAVENSCHLAG, K., SCHUBERT, C. J., RICKERT, D., WIDDEL, F., GIESEKE, A., AMANN, R., JØRGENSEN, B. B., WITTE, U. & PFANNKUCHE, O. 2000b. A marine microbial consortium apparently mediating anaerobic oxidation of methane. *Nature,* 407**,** 623-626.

CAFFREY, S. M. & VOORDOUW, G. 2010. Effect of sulfide on growth physiology and gene expression of Desulfovibrio vulgaris Hildenborough. *Antonie Van Leeuwenhoek,* 97**,** 11-20.

CALLAGHAN, A. V. 2013. Enzymes involved in the anaerobic oxidation of n-alkanes: from methane to long-chain paraffins. *Frontiers in Microbiology,* 4.

CASTRESANA, J. 2000. Selection of conserved blocks from multiple alignments for their use in phylogenetic analysis. *Mol Biol Evol,* 17**,** 540-52.

COSTA, K. C. & LEIGH, J. A. 2014. Metabolic versatility in methanogens. *Curr Opin Biotechnol,* 29**,** 70-5.

CRANE, B. R. & GETZOFF, E. D. 1996. The relationship between structure and function for the sulfite reductases. *Current Opinion in Structural Biology,* 6**,** 744-756.

CUI, M., MA, A., QI, H., ZHUANG, X. & ZHUANG, G. 2015. Anaerobic oxidation of methane: an "active" microbial process. *Microbiologyopen,* 4**,** 1-11.

DAHLE, H., OKLAND, I., THORSETH, I. H., PEDERESEN, R. B. & STEEN, I. H. 2015. Energy landscapes shape microbial communities in hydrothermal systems on the Arctic Mid-Ocean Ridge. *Isme j,* 9**,** 1593-606.

DEKAS, A. E., CHADWICK, G. L., BOWLES, M. W., JOYE, S. B. & ORPHAN, V. J. 2014. Spatial distribution of nitrogen fixation in methane seep sediment and the role of the ANME archaea. *Environ Microbiol,* 16**,** 3012-29.

DEKAS, A. E., PORETSKY, R. S. & ORPHAN, V. J. 2009. Deep-sea archaea fix and share nitrogen in methane-consuming microbial consortia. *Science,* 326**,** 422-6.

DEREEPER, A., GUIGNON, V., BLANC, G., AUDIC, S., BUFFET, S., CHEVENET, F., DUFAYARD, J. F., GUINDON, S., LEFORT, V., LESCOT, M., CLAVERIE, J. M. & GASCUEL, O. 2008. Phylogeny.fr: robust phylogenetic analysis for the non-specialist. *Nucleic Acids Res,* 36**,** W465-9.

EDGAR, R. C. 2004. MUSCLE: multiple sequence alignment with high accuracy and high throughput. *Nucleic Acids Res,* 32**,** 1792-7.

ELLEFSON, W. L. & WOLFE, R. S. 1981. Component C of the methylreductase system of Methanobacterium. *J Biol Chem,* 256**,** 4259-62.

ERMLER, U., GRABARSE, W., SHIMA, S., GOUBEAUD, M. & THAUER, R. K. 1997. Crystal structure of methyl-coenzyme M reductase: the key enzyme of biological methane formation. *Science,* 278**,** 1457-62.

ETTWIG, K. F., BUTLER, M. K., LE PASLIER, D., PELLETIER, E., MANGENOT, S., KUYPERS, M. M., SCHREIBER, F., DUTILH, B. E., ZEDELIUS, J., DE BEER, D., GLOERICH, J., WESSELS, H. J., VAN ALEN, T., LUESKEN, F., WU, M. L., VAN DE PAS-SCHOONEN, K. T., OP DEN CAMP, H. J., JANSSEN-MEGENS, E. M., FRANCOIJS, K. J., STUNNENBERG, H., WEISSENBACH, J., JETTEN, M. S. & STROUS, M. 2010. Nitrite-driven anaerobic methane oxidation by oxygenic bacteria. *Nature,* 464**,** 543-8.

FRITZ, G., ROTH, A., SCHIFFER, A., BUCHERT, T., BOURENKOV, G., BARTUNIK, H. D., HUBER, H., STETTER, K. O., KRONECK, P. M. & ERMLER, U. 2002. Structure of adenylylsulfate reductase from the hyperthermophilic Archaeoglobus fulgidus at 1.6-A resolution. *Proc Natl Acad Sci U S A,* 99**,** 1836-41.

FUCHS, G. 2011. Alternative pathways of carbon dioxide fixation: insights into the early evolution of life? *Annu Rev Microbiol,* 65**,** 631-58.

GRABARSE, W., MAHLERT, F., SHIMA, S., THAUER, R. K. & ERMLER, U. 2000. Comparison of three methyl-coenzyme M reductases from phylogenetically distant organisms: unusual amino acid modification, conservation and adaptation. *J Mol Biol,* 303**,** 329-44.

GREIN, F., RAMOS, A. R., VENCESLAU, S. S. & PEREIRA, I. A. C. 2013. Unifying concepts in anaerobic respiration: Insights from dissimilatory sulfur metabolism. *Biochimica et Biophysica Acta (BBA) - Bioenergetics,* 1827**,** 145-160.

H. D. PECK, J. 1962. Comparative metabolism of inorganic sulfur compounds in microorganisms. *Microbiol. Mol. Biol. Rev.,* 26**,** 67-94.

HALLAM, S. J., GIRGUIS, P. R., PRESTON, C. M., RICHARDSON, P. M. & DELONG, E. F. 2003. Identification of methyl coenzyme M reductase A (mcrA) genes associated with methane-oxidizing archaea. *Appl Environ Microbiol,* 69**,** 5483-91.

HALLAM, S. J., PUTNAM, N., PRESTON, C. M., DETTER, J. C., ROKHSAR, D., RICHARDSON, P. M. & DELONG, E. F. 2004. Reverse methanogenesis: testing the hypothesis with environmental genomics. *Science,* 305**,** 1457-62.

HANDELSMAN, J. 2004. Metagenomics: application of genomics to uncultured microorganisms. *Microbiol Mol Biol Rev,* 68**,** 669-85.

HANSEN, T. A. 1994. Metabolism of sulfate-reducing prokaryotes. *Antonie Van Leeuwenhoek,* 66**,** 165-85.

HAROON, M. F., HU, S., SHI, Y., IMELFORT, M., KELLER, J., HUGENHOLTZ, P., YUAN, Z. & TYSON, G. W. 2013a. Anaerobic oxidation of methane coupled to nitrate reduction in a novel archaeal lineage. *Nature,* 500**,** 567-570.

HAROON, M. F., HU, S., SHI, Y., IMELFORT, M., KELLER, J., HUGENHOLTZ, P., YUAN, Z. & TYSON, G. W. 2013b. Anaerobic oxidation of methane coupled to nitrate reduction in a novel archaeal lineage. *Nature,* 500**,** 567-70.

HAWLEY, E. R., PIAO, H., SCOTT, N. M., MALFATTI, S., PAGANI, I., HUNTEMANN, M., CHEN, A., GLAVINA DEL RIO, T., FOSTER, B., COPELAND, A., JANSSON, J., PATI, A., GILBERT, J. A., TRINGE, S., LORENSON, T. D. & HESS, M. 2014. *Metagenomic analysis of microbial consortium from natural crude oil that seeps into the marine ecosystem offshore Southern California*.

HOVLAND, M., SVENSEN, H., FORSBERG, C. F., JOHANSEN, H., FICHLER, C., FOSSÅ, J. H., JONSSON, R. & RUESLÅTTEN, H. 2005. Complex pockmarks with carbonate-ridges off mid-Norway: Products of sediment degassing. *Marine Geology,* 218**,** 191-206.

HUGLER, M. & SIEVERT, S. M. 2011. Beyond the Calvin cycle: autotrophic carbon fixation in the ocean. *Ann Rev Mar Sci,* 3**,** 261-89.

HUSON, D. H., MITRA, S., RUSCHEWEYH, H. J., WEBER, N. & SCHUSTER, S. C. 2011. Integrative analysis of environmental sequences using MEGAN4. *Genome Res,* 21**,** 1552-60.

HYATT, D., CHEN, G. L., LOCASCIO, P. F., LAND, M. L., LARIMER, F. W. & HAUSER, L. J. 2010. Prodigal: prokaryotic gene recognition and translation initiation site identification. *BMC Bioinformatics,* 11**,** 119.

IVANOV, M., MAZZINI, A., BLINOVA, V., KOZLOVA, E., LABERG, J.-S., MATVEEVA, T., TAVIANI, M. & KASKOV, N. 2010. Seep mounds on the Southern Vøring Plateau (offshore Norway). *Marine and Petroleum Geology,* 27**,** 1235-1261.

IVERSEN, N. & JORGENSEN, B. B. 1985. Anaerobic Methane Oxidation Rates at the Sulfate-Methane Transition in Marine Sediments from Kattegat and Skagerrak (Denmark). *Limnology and Oceanography,* 30**,** 944-955.

JORGENSEN, B. B. & BOETIUS, A. 2007. Feast and famine--microbial life in the deep-sea bed. *Nat Rev Microbiol,* 5**,** 770-81.

KELLER, K. L. & WALL, J. D. 2011. Genetics and molecular biology of the electron flow for sulfate respiration in desulfovibrio. *Front Microbiol,* 2**,** 135.

KELLERMANN, M. Y., WEGENER, G., ELVERT, M., YOSHINAGA, M. Y., LIN, Y. S., HOLLER, T., MOLLAR, X. P., KNITTEL, K. & HINRICHS, K. U. 2012. Autotrophy as a predominant mode of carbon fixation in anaerobic methane-oxidizing microbial communities. *Proc Natl Acad Sci U S A,* 109**,** 19321-6.

KELLEY, D. S. & FRÜH-GREEN, G. L. 1999. Abiogenic methane in deep-seated mid-ocean ridge environments: Insights from stable isotope analyses. *Journal of Geophysical Research: Solid Earth,* 104**,** 10439-10460.

KIETAVAINEN, R. & PURKAMO, L. 2015. The origin, source, and cycling of methane in deep crystalline rock biosphere. *Front Microbiol,* 6**,** 725.

KNITTEL, K. & BOETIUS, A. 2009. Anaerobic oxidation of methane: progress with an unknown process. *Annu Rev Microbiol,* 63**,** 311-34.

KNITTEL, K., LOSEKANN, T., BOETIUS, A., KORT, R. & AMANN, R. 2005. Diversity and distribution of methanotrophic archaea at cold seeps. *Appl Environ Microbiol,* 71**,** 467-79.

KRUGER, M., MEYERDIERKS, A., GLOCKNER, F. O., AMANN, R., WIDDEL, F., KUBE, M., REINHARDT, R., KAHNT, J., BOCHER, R., THAUER, R. K. & SHIMA, S. 2003. A conspicuous nickel protein in microbial mats that oxidize methane anaerobically. *Nature,* 426**,** 878-81.

KVENVOLDEN, K. A. 1993. Gas hydrates—geological perspective and global change. *Reviews of Geophysics,* 31**,** 173-187.

KVENVOLDEN, K. A. & ROGERS, B. W. 2005. Gaia's breath—global methane exhalations. *Marine and Petroleum Geology,* 22**,** 579-590.

LADOUKAKIS, E., KOLISIS, F. N. & CHATZIIOANNOU, A. A. 2014. Integrative workflows for metagenomic analysis. *Front Cell Dev Biol,* 2**,** 70.

LEIGH, J. A. 2000. Nitrogen fixation in methanogens: the archaeal perspective. *Curr Issues Mol Biol,* 2**,** 125-31.

LETUNIC, I. & BORK, P. 2011. Interactive Tree Of Life v2: online annotation and display of phylogenetic trees made easy. *Nucleic Acids Res,* 39**,** W475-8.

LIU, Y. & WHITMAN, W. B. 2008. Metabolic, phylogenetic, and ecological diversity of the methanogenic archaea. *Ann N Y Acad Sci,* 1125**,** 171-89.

LJUNGDAHL, L. G. 1986. The autotrophic pathway of acetate synthesis in acetogenic bacteria. *Annu Rev Microbiol,* 40**,** 415-50.

LLOYD, K. G., ALPERIN, M. J. & TESKE, A. 2011. Environmental evidence for net methane production and oxidation in putative ANaerobic MEthanotrophic (ANME) archaea. *Environmental Microbiology,* 13**,** 2548-2564.

MADIGAN, M. T., MARTINKO, J. M., BROCK, T. D., BENDER, K. S., BUCKLEY, D. H. & STAHL, D. A. 2015. *Brock biology of microorganisms,* Harlow, Pearson.

MADIGAN, M. T., MARTINKO, J. M., STAHL, D. A. & CLARK, D. P. 2011. *Biology of microorganisms*.

MARDIS, E. R. 2008. Next-generation DNA sequencing methods. *Annu Rev Genomics Hum Genet,* 9**,** 387-402.

MARKOWITZ, V. M., CHEN, I. M., PALANIAPPAN, K., CHU, K., SZETO, E., PILLAY, M., RATNER, A., HUANG, J., WOYKE, T., HUNTEMANN, M., ANDERSON, I., BILLIS, K., VARGHESE, N., MAVROMATIS, K., PATI, A., IVANOVA, N. N. & KYRPIDES, N. C. 2014. IMG 4 version of the integrated microbial genomes comparative analysis system. *Nucleic Acids Res,* 42**,** D560-7.

MAZZINI, A., SVENSEN, H., HOVLAND, M. & PLANKE, S. 2006. Comparison and implications from strikingly different authigenic carbonates in a Nyegga complex pockmark, G11, Norwegian Sea. *Marine Geology,* 231**,** 89-102.

MEULEPAS, R. J., JAGERSMA, C. G., KHADEM, A. F., STAMS, A. J. & LENS, P. N. 2010. Effect of methanogenic substrates on anaerobic oxidation of methane and sulfate reduction by an anaerobic methanotrophic enrichment. *Appl Microbiol Biotechnol,* 87**,** 1499-506.

MEYERDIERKS, A., KUBE, M., KOSTADINOV, I., TEELING, H., GLOCKNER, F. O., REINHARDT, R. & AMANN, R. 2010. Metagenome and mRNA expression analyses of anaerobic methanotrophic archaea of the ANME-1 group. *Environ Microbiol,* 12**,** 422-39.

MEYERDIERKS, A., KUBE, M., LOMBARDOT, T., KNITTEL, K., BAUER, M., GLOCKNER, F. O., REINHARDT, R. & AMANN, R. 2005. Insights into the genomes of archaea mediating the anaerobic oxidation of methane. *Environ Microbiol,* 7**,** 1937-51.

MILLER, J. R., KOREN, S. & SUTTON, G. 2010. Assembly algorithms for next-generation sequencing data. *Genomics,* 95**,** 315-27.

MILLS, H. J., HODGES, C., WILSON, K., MACDONALD, I. R. & SOBECKY, P. A. 2003. Microbial diversity in sediments associated with surface-breaching gas hydrate mounds in the Gulf of Mexico. *FEMS Microbiol Ecol,* 46**,** 39-52.

MILUCKA, J., FERDELMAN, T. G., POLERECKY, L., FRANZKE, D., WEGENER, G., SCHMID, M., LIEBERWIRTH, I., WAGNER, M., WIDDEL, F. & KUYPERS, M. M. M. 2012. Zero-valent sulphur is a key intermediate in marine methane oxidation. *Nature,* 491**,** 541-546.

MIZUNO, N., VOORDOUW, G., MIKI, K., SARAI, A. & HIGUCHI, Y. 2003. Crystal Structure of Dissimilatory Sulfite Reductase D (DsrD) Protein—Possible Interaction with B- and Z-DNA by Its Winged-Helix Motif. *Structure,* 11**,** 1133-1140.

MORAN, J. J., BEAL, E. J., VRENTAS, J. M., ORPHAN, V. J., FREEMAN, K. H. & HOUSE, C. H. 2008. Methyl sulfides as intermediates in the anaerobic oxidation of methane. *Environ Microbiol,* 10**,** 162-73.

MOUNT, D. W. 2007. Steps Used by the BLAST Algorithm. *CSH Protoc,* 2007**,** pdb.ip41.

NAUHAUS, K., BOETIUS, A., KRUGER, M. & WIDDEL, F. 2002. In vitro demonstration of anaerobic oxidation of methane coupled to sulphate reduction in sediment from a marine gas hydrate area. *Environ Microbiol,* 4**,** 296-305.

NAUHAUS, K., TREUDE, T., BOETIUS, A. & KRUGER, M. 2005. Environmental regulation of the anaerobic oxidation of methane: a comparison of ANME-I and ANME-II communities. *Environ Microbiol,* 7**,** 98-106.

NIEMANN, H., LOSEKANN, T., DE BEER, D., ELVERT, M., NADALIG, T., KNITTEL, K., AMANN, R., SAUTER, E. J., SCHLUTER, M., KLAGES, M., FOUCHER, J. P. & BOETIUS, A. 2006. Novel microbial communities of the Haakon Mosby mud volcano and their role as a methane sink. *Nature,* 443**,** 854-8.

OLIVEIRA, T. F., VONRHEIN, C., MATIAS, P. M., VENCESLAU, S. S., PEREIRA, I. A. C. & ARCHER, M. 2008. The Crystal Structure of Desulfovibrio vulgaris Dissimilatory Sulfite Reductase Bound to DsrC Provides Novel Insights into the Mechanism of Sulfate Respiration. *The Journal of Biological Chemistry,* 283**,** 34141-34149.

ORCUTT, B. N., SYLVAN, J. B., KNAB, N. J. & EDWARDS, K. J. 2011. Microbial ecology of the dark ocean above, at, and below the seafloor. *Microbiol Mol Biol Rev,* 75**,** 361-422.

ORPHAN, V. J., HOUSE, C. H., HINRICHS, K. U., MCKEEGAN, K. D. & DELONG, E. F. 2001. Methane-consuming archaea revealed by directly coupled isotopic and phylogenetic analysis. *Science,* 293**,** 484-7.

ORPHAN, V. J., HOUSE, C. H., HINRICHS, K. U., MCKEEGAN, K. D. & DELONG, E. F. 2002. Multiple archaeal groups mediate methane oxidation in anoxic cold seep sediments. *Proc Natl Acad Sci U S A,* 99**,** 7663-8.

OVERBEEK, R., OLSON, R., PUSCH, G. D., OLSEN, G. J., DAVIS, J. J., DISZ, T., EDWARDS, R. A., GERDES, S., PARRELLO, B., SHUKLA, M., VONSTEIN, V., WATTAM, A. R., XIA, F. & STEVENS, R. 2014. The SEED and the Rapid Annotation of microbial genomes using Subsystems Technology (RAST). *Nucleic Acids Res,* 42**,** D206-14.

PAUL, K., NONOH, J. O., MIKULSKI, L. & BRUNE, A. 2012. "Methanoplasmatales," Thermoplasmatales-related archaea in termite guts and other environments, are the seventh order of methanogens. *Appl Environ Microbiol,* 78**,** 8245-53.

RAMOS, A. R., KELLER, K. L., WALL, J. D. & PEREIRA, I. A. 2012. The Membrane QmoABC Complex Interacts Directly with the Dissimilatory Adenosine 5'-Phosphosulfate Reductase in Sulfate Reducing Bacteria. *Front Microbiol,* 3**,** 137.

REEBURGH, W. S. 2007. Oceanic methane biogeochemistry. *Chem Rev,* 107**,** 486-513.

ROALKVAM, I., JORGENSEN, S. L., CHEN, Y., STOKKE, R., DAHLE, H., HOCKING, W. P., LANZEN, A., HAFLIDASON, H. & STEEN, I. H. 2011. New insight into stratification of anaerobic methanotrophs in cold seep sediments. *FEMS Microbiol Ecol,* 78**,** 233-43.

RONAGHI, M., UHLEN, M. & NYREN, P. 1998. A sequencing method based on real-time pyrophosphate. *Science,* 281**,** 363, 365.

RUSK, N. 2011. Torrents of sequence. *Nat Meth,* 8**,** 44-44.

SANGER, F., NICKLEN, S. & COULSON, A. R. 1977. DNA sequencing with chain-terminating inhibitors. *Proc Natl Acad Sci U S A,* 74**,** 5463-7.

SCHAUDER, R., WIDDEL, F. & FUCHS, G. 1987. Carbon assimilation pathways in sulfate-reducing bacteria II. Enzymes of a reductive citric acid cycle in the autotrophic Desulfobacter hydrogenophilus. *Archives of Microbiology,* 148**,** 218-225.

SHERWOOD LOLLAR, B., WESTGATE, T. D., WARD, J. A., SLATER, G. F. & LACRAMPE-COULOUME, G. 2002. Abiogenic formation of alkanes in the Earth's crust as a minor source for global hydrocarbon reservoirs. *Nature,* 416**,** 522-4.

SHIMA, S., KRUEGER, M., WEINERT, T., DEMMER, U., KAHNT, J., THAUER, R. K. & ERMLER, U. 2012. Structure of a methyl-coenzyme M reductase from Black Sea mats that oxidize methane anaerobically. *Nature,* 481**,** 98-101.

SIEGL, A., KAMKE, J., HOCHMUTH, T., PIEL, J., RICHTER, M., LIANG, C., DANDEKAR, T. & HENTSCHEL, U. 2011. Single-cell genomics reveals the lifestyle of Poribacteria, a candidate phylum symbiotically associated with marine sponges. *Isme j,* 5**,** 61-70.

SIQUEIRA, J. F., JR., FOUAD, A. F. & ROCAS, I. N. 2012. Pyrosequencing as a tool for better understanding of human microbiomes. *J Oral Microbiol,* 4.

SPRING, S., NOLAN, M., LAPIDUS, A., GLAVINA DEL RIO, T., COPELAND, A., TICE, H., CHENG, J. F., LUCAS, S., LAND, M., CHEN, F., BRUCE, D., GOODWIN, L., PITLUCK, S., IVANOVA, N., MAVROMATIS, K., MIKHAILOVA, N., PATI, A., CHEN, A., PALANIAPPAN, K., HAUSER, L., CHANG, Y. J., JEFFRIES, C. D., MUNK, C., KISS, H., CHAIN, P., HAN, C., BRETTIN, T., DETTER, J. C., SCHULER, E., GOKER, M., ROHDE, M., BRISTOW, J., EISEN, J. A., MARKOWITZ, V., HUGENHOLTZ, P., KYRPIDES, N. C. & KLENK, H. P. 2010. Complete genome sequence of Desulfohalobium retbaense type strain (HR(100)). *Stand Genomic Sci,* 2**,** 38-48.

STATES, D. J. & GISH, W. 1994. Combined use of sequence similarity and codon bias for coding region identification. *J Comput Biol,* 1**,** 39-50.

STOKKE, R., ROALKVAM, I., LANZEN, A., HAFLIDASON, H. & STEEN, I. H. 2012. Integrated metagenomic and metaproteomic analyses of an ANME-1-dominated community in marine cold seep sediments. *Environ Microbiol,* 14**,** 1333-46.

STROUS, M., KRAFT, B., BISDORF, R. & TEGETMEYER, H. 2012a. The binning of metagenomic contigs for microbial physiology of mixed cultures. *Frontiers in Microbiology,* 3.

STROUS, M., KRAFT, B., BISDORF, R. & TEGETMEYER, H. E. 2012b. The binning of metagenomic contigs for microbial physiology of mixed cultures. *Front Microbiol,* 3**,** 410.

TAGUCHI, Y., SUGISHIMA, M. & FUKUYAMA, K. 2004. Crystal structure of a novel zinc-binding ATP sulfurylase from Thermus thermophilus HB8. *Biochemistry,* 43**,** 4111-8.

TAMURA, K., DUDLEY, J., NEI, M. & KUMAR, S. 2007. MEGA4: Molecular Evolutionary Genetics Analysis (MEGA) software version 4.0. *Mol Biol Evol,* 24**,** 1596-9.

THAUER, R. K., KASTER, A. K., SEEDORF, H., BUCKEL, W. & HEDDERICH, R. 2008. Methanogenic archaea: ecologically relevant differences in energy conservation. *Nat Rev Microbiol,* 6**,** 579-91.

WANG, F. P., ZHANG, Y., CHEN, Y., HE, Y., QI, J., HINRICHS, K. U., ZHANG, X. X., XIAO, X. & BOON, N. 2014. Methanotrophic archaea possessing diverging methane-oxidizing and electron-transporting pathways. *Isme j,* 8**,** 1069-78.

WEGENER, G., NIEMANN, H., ELVERT, M., HINRICHS, K. U. & BOETIUS, A. 2008. Assimilation of methane and inorganic carbon by microbial communities mediating the anaerobic oxidation of methane. *Environ Microbiol,* 10**,** 2287-98.

WOESE, C. R. 1987. Bacterial evolution. *Microbiol Rev,* 51**,** 221-71.

WOOD, H. G. 1991. Life with CO or CO2 and H2 as a source of carbon and energy. *Faseb j,* 5**,** 156-63.

YOK, N. & ROSEN, G. 2010. Benchmarking of gene prediction programs for metagenomic data. *Conf Proc IEEE Eng Med Biol Soc,* 2010**,** 6190-3.

ZEPEDA MENDOZA, M. L., SICHERITZ-PONTEN, T. & GILBERT, M. T. 2015. Environmental genes and genomes: understanding the differences and challenges in the approaches and software for their analyses. *Brief Bioinform*.

ZOBELL, C. E. & MORITA, R. 1959. Deep-sea bacteria. *Galathea Report, Danish Science, Copenhagen,* 1**,** 139-154.

Appendix

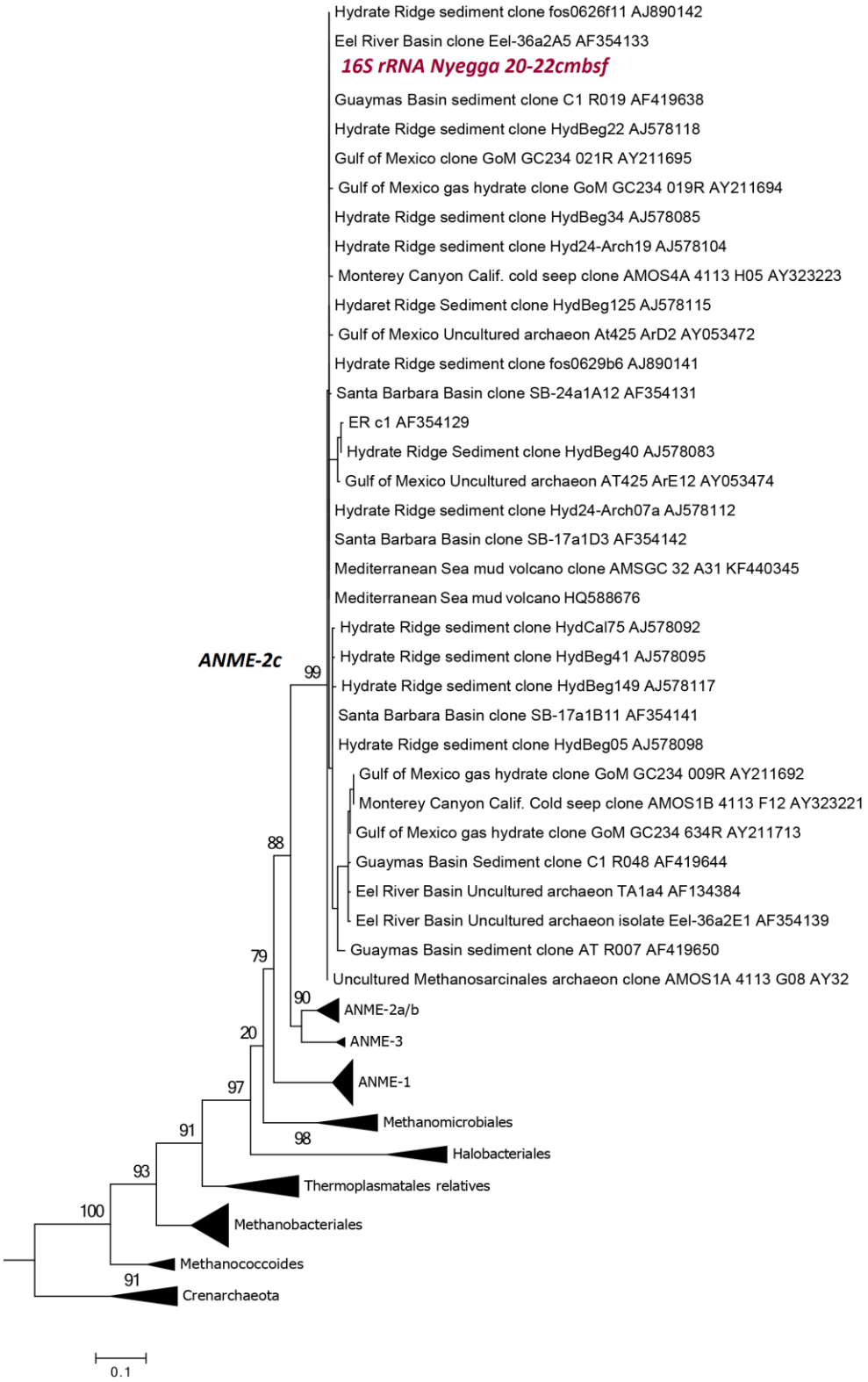

Appendix I. phylogenetic tree of 16SrRNA sequences, including 16S rRNA in contig01666 from the Nyegga sediment at 20-22cmbsf. The tree is based on a MUSCLE alignment and constructed with the PhyML program using 100 bootstrap values

Appendix II. List of selected McrA sequences and their accession NO.

No.	species	Accsesion No.
1	*Methanomethylovorans hollandica*	WP_015325028.1
2	*Candidatus Methanoperedens nitroreducens*	KCZ72673
3	uncultured archaeon GZfos35D7	AAQ63481.1
4	uncultured archaeon GZfos26B2	AAU83007
5	*Black sea uncultured archaeon*	CAE46369
6	uncultured archaeon GZfos24D9	AAU82960
7	uncultured archaeon GZfos30H9	AAU83544
8	*Black sea-uncultured archaeon*	CBH39484
9	uncultured archaeon GZfos11H11	AAU82226
10	uncultured archaeon GZfos18B6	AAU82491
11	uncultured archaeon GZfos9C4	AAU84252
12	uncultured archaeon GZfos19C7	AAU82711
13	uncultured archaeon GZfos13E1	AAU82276
14	Eel River Basin- uncultured archaeon	AAQ63476
15	*Methanocaldococcus vulcanius M7*	WP_012819563
16	*Methanocaldococcus infernus ME*	ZP_04790423
17	*Methanobrevibacter smithii DSM 2375*	ZP_03607827
18	*Methanocella arvoryzae*	WP_012035370
19	*Methanoregula boonei*	WP_012106121
20	*Methanobacterium paludisgi*	WP_013826564.1
21	*Methanocaldococcus fervens AG86*	WP_015791493
22	*Methanocaldococcus jannaschii DSM 2661*	NP_247840
23	*Methanococcus aeolicus Nankai-3*	WP_011973976
24	*Methanocorpusculum labreanum Z*	WP_011833928
25	*Methanothermobacter thermautotrophicus str. Delta H*	WP_010876788
26	*Methanosphaerula palustris E1-9c*	WP_012618913
27	*Methanococcus maripaludis S2*	WP_011171503
28	*Methanococcus vannielii SB*	WP_011972678
29	*Methanosaeta thermophila PT*	YP_843000
30	*Methanothermobacter marburgensis*	WP_013296337
31	*Methanococcus voltae A3*	ZP_02193000
32	*Methanosarcina mazei Go1*	WP_011033189
33	*Methanosarcina acetivorans C2A*	WP_011024419
34	*Methanosarcina barkeri str. Fusaro*	WP_011305916
35	*Methanoculleus marisnigri JR1*	WP_011843456
36	*Methanococcoides burtonii DSM 6242*	WP_011500403

Appendix III. List of selected AprBA sequences and their accession NO .

No.	Species	AprA Accession number	AprB Accession number
1	*Chlorobium tepidum TLS*	NP_661759.1	NP_661758.1
2	*Chlorobium phaeobacteroides BS1*	ACE04754.1	YP_001960236.1
3	*Chlorobium chlorochromatii CaD3*	YP_379883.1	YP_379884.1
4	uncultured alpha proteobacterium EBAC2C11	AAV31646.1	AAV31645.1
5	Thiobacillus denitrificans ATCC 25259	YP_314630.1	YP_316041.1
6	*T*hiobacillus *denitrificans ATCC 25259*	YP_316040.1	YP_314631.1
7	*Allochromatium vinosum DSM 180*	AAC23621.1	YP_003443091.1
8	*Desulfotalea psychrophila LSv54*	YP_064841.1	YP_064840.1
9	*Desulfovibrio vulgaris str. Hildenborough*	YP_010068.1	YP_010067.1
10	*Desulfovibrio desulfuricans subsp. desulfuricans str. G20*	YP_387606.1	YP_387605.1
11	*Syntrophobacter fumaroxidans MPOB*	YP_845177.1	YP_845176.1
12	*uncultured sulfate-reducing bacterium fosws39f7*	CAJ31180.1	CAJ31179.1
13	*Thermodesulfobacterium commune DSM 2178*	ABR92412.1	ABR92411.1
14	*Thermodesulfobacterium hveragerdense*	ABR92414.1	ABR92413.1
15	*Thermodesulfovibrio yellowstonii DSM 11347*	YP_002249623.1	YP_002249624.1
16	*Desulfotomaculum nigrificans DSM 574*	ZP_08112930.1	ZP_08112929.1
17	*Desulfotomaculum acetoxidans DSM 771*	YP_003192912.1	YP_003192913.1
18	*Desulfotomaculum reducens MI-1*	YP_001112002.1	YP_001112001.1
19	*Archaeoglobus veneficus SNP6*	YP_004341170.1	YP_004341169.1
20	*Archaeoglobus profundus DSM 5631*	YP_003400986.1	YP_003400987.1
21	*Archaeoglobus fulgidus DSM 4304*	NP_070498.1	NP_070497.1
22	*Caldivirga maquilingensis IC-167*	YP_001540111.1	YP_001540110.1
23	*Pyrobaculum arsenaticum DSM 13514*	ABP50802.1	ABP50801.1
24	*Pyrobaculum calidifontis JCM 11548*	ABO08848.1	ABO08849.1
25	*Desulfobacterium autotrophicum HRM2*	YP_002601730.1	YP_002601731.1
26	*Desulfococcus oleovorans Hxd3*	YP_001528885.1	YP_001528884.1
27	*Desulfohalobium retbaense DSM 5692*	YP_003198828.1	YP_003198829.1
28	*Desulfovibrio salexigens DSM 2638*	YP_002989836.1	YP_002989835.1
29	*Desulfovibrio magneticus RS-1*	YP_002951917.1	YP_002951916.1
30	*Thioalkalivibrio sulfidophilus HL-EbGr7*	YP_002512435.1	YP_002512436.1
31	*Desulfovibrio desulfuricans subsp. desulfuricans str. ATCC 27774*	YP_002480703.1	YP_002480704.1
32	*Desulfovibrio vulgaris str. 'Miyazaki F'*	YP_002437297.1	YP_002437298.1
33	*Desulfatibacillum alkenivorans AK-01*	YP_002430735.1	YP_002430736.1
34	*Candidatus Desulforudis audaxviator MP104C*	YP_001718010.1	YP_001718011.1
35	*Candidatus Vesicomyosocius okutanii HA*	YP_001218952.1	YP_001218951.1
36	*Desulfovibrio vulgaris DP4*	YP_967579.1	YP_967580.1
37	*Candidatus Pelagibacter ubique HTCC1062*	YP_266257.1	YP_266256.1
38	*Desulfosarcina cetonica*	AEG42204.1	AEG42203.1

39	*Desulfosarcina ovata*	AEG42192.1	AEG42191.1
40	*Desulfobacterium anilini*	ABR92539.1	ABR92538.1
41	*Desulfarculus baarsii*	ABR92547.1	ABR92546.1
42	*Desulfomonile tiedjei DSM 6799*	ABR92551.1	ABR92550.1
43	*Thermodesulfatator indicus DSM 15286*	YP_004625133.1	YP_004625134.1
44	*Desulfobacca acetoxidans DSM 11109*	YP_004369796.1	YP_004369797.1
45	*Desulfobulbus propionicus DSM 2032*	YP_004194237.1	YP_004194236.1
46	*Vulcanisaeta distributa DSM 14429*	YP_003902509.1	YP_003902510.1
47	*Thermodesulfobium narugense DSM 14796*	YP_004438339.1	YP_004438340.1
48	*Sideroxydans lithotrophicus ES-1*	YP_003524335.1	YP_003524334.1
49	*Ammonifex degensii KC4*	YP_003239057.1	YP_003239058.1
50	*Desulfovibrio aespoeensis Aspo-2*	YP_004122772.1	YP_004122773.1
51	*Desulfomicrobium baculatum DSM 4028*	YP_003159689.1	YP_003159688.1
52	*Pelodictyon phaeoclathratiforme BU-1*	YP_002017013.1	YP_002017014.1
53	*Thioalkalivibrio sp. K90mix*	YP_003459318.1	YP_003459317.1
54	*Thioalkalivibrio thiocyanoxidans ARh 4*	ZP_08928668.1	ZP_08928669.1
55	*Desulfonatronospira thiodismutans ASO3-1*	ZP_07016333.1	ZP_07016332.1
56	*Desulfovibrio sp. ND132*	ZP_08111962.1	ZP_08111961.1
57	*Candidatus Ruthia magnifica str. Cm (Calyptogena magnifica)*	YP_903358.1	YP_903357.1
58	*Thermodesulfobacterium sp. OPB45*	YP_004627219.1	YP_004627220.1
59	*Desulfotomaculum kuznetsovii DSM 6115*	YP_004516462.1	YP_004516461.1
60	*Desulfovibrio alaskensis G20*	YP_387606.1	YP_387605.1
61	*Desulfotomaculum carboxydivorans CO-1-SRB*	YP_004498124.1	YP_004498125.1
62	*Desulfovibrio sp. FW1012B*	ZP_09131868.1	ZP_09131867.1
63	*Desulfotomaculum gibsoniae DSM 7213*	ZP_09099083.1	ZP_09099084.1
64	*Desulfobacter postgatei 2ac9*	ZP_09095985.1	ZP_09095984.1
65	*Desulfosporosinus meridiei DSM 13257*	ZP_08983439.1	ZP_08983440.1
66	*Thiorhodovibrio sp. 970*	ZP_08943161.1	ZP_08943162.1
67	*Thiocystis violascens DSM 198*	ZP_08926409.1	ZP_08926410.1
68	*Thiorhodococcus drewsii AZ1*	ZP_08823264.1	ZP_08823265.1
69	*Thiorhodococcus drewsii AZ1*	ZP_08822682.1	ZP_08822681.1
70	*Thiocapsa marina 5811*	ZP_08772813.1	ZP_08772812.1
71	*Desulfovibrio fructosovorans JJ*	ZP_07334194.1	ZP_07334195.1
72	*Desulfovibrio africanus str. Walvis Bay*	ZP_08421590.1	ZP_08421591.1
73	*Desulfurivibrio alkaliphilus AHT2*	YP_003690785.1	YP_003690786.1
74	*Thermoproteus uzoniensis 768-20*	YP_004337517.1	YP_004337516.1
75	*Vulcanisaeta moutnovskia 768-28*	YP_004244206.1	YP_004244207.1
76	*gamma proteobacterium SCGC AAA001-B15*	ZP_09063649.1	ZP_09063648.1
77	*Thermoproteus tenax Kra 1*	YP_004892186.1	YP_004892187.1
78	*Desulfovibrio sp. A2*	ZP_08867105.1	ZP_08867106.1
79	*Desulfovibrio sp. 6_1_46AFAA*	ZP_08842825.1	ZP_08842824.1
80	*delta proteobacterium MLMS-1*	ZP_01288427.1	ZP_01288426.1
81	*endosymbiont of Tevnia jerichonana (vent Tica)*	ZP_08816020.1	ZP_08816021.1
82	*sulfate-reducing bacterium DSM 12567*	ABR92545.1	ABR92544.1

83	*sulfate-reducing bacterium DSM 15769*	ABR92541.1	ABR92540.1
84	*sulfate-reducing bacterium DSM 14454*	ABR92543.1	ABR92542.1
85	*Desulforhabdus sp. DDT*	ABR92557.1	ABR92556.1
86	*Desulforhabdus amnigena*	ABR92553.1	ABR92552.1
87	*Desulforhabdus sp. BKA11*	ABR92555.1	ABR92554.1
88	*Desulfotomaculum sp. DSM 8775*	ABR92586.1	ABR92585.1
89	*Desulfotomaculum thermocisternum*	ABR92594.1	ABR92593.1
90	*Desulfotomaculum luciae*	ABR92571.1	ABR92570.1
91	*Desulfotomaculum australicum*	ABR92565.1	ABR92564.1
92	*Desulfotomaculum solfataricum*	ABR92576.1	ABR92575.1
93	*Desulfotomaculum thermobenzoicum subsp. thermobenzoicum*	ABR92590.1	ABR92589.1
94	*Desulfotomaculum sp. DSM 7475*	ABR92582.1	ABR92581.1
95	*Desulfotomaculum sp. DSM 7474*	ABR92580.1	ABR92579.1
96	*Desulfotomaculum sp. DSM 7476*	ABR92584.1	ABR92583.1
97	*Desulfotomaculum thermobenzoicum subsp. thermosyntrophicum*	ABR92592.1	ABR92591.1
98	*uncultured sulfate-reducing bacterium*	CAJ31201.1	CAJ31202.1
99	*Desulfotomaculum sp. DSM 7440*	ABR92578.1	ABR92577.1
100	*Desulfosporosinus orientis DSM 765*	AET67375.1	AET67374.1
101	*Desulfonatronovibrio hydrogenovorans*	ABR92460.1	ABR92459.1
102	*Desulfothermus naphthae*	ABR92458.1	ABR92457.1
103	*BS_Apr1_Black_Sea*	AEG42194.1	AEG42193.1
104	*BS_Apr2_Black_Sea*	AEG42196.1	AEG42195.1
105	*BS_Apr3_Black_Sea*	AEG42198.1	AEG42197.1
106	*BS_Apr4_Black_Sea*	AEG42200.1	AEG42199.1
107	*BS_Apr5_Black_Sea*	AEG42202.1	AEG42201.1

Appendix IV. List of selected 16S rRNA sequences and their accession no.

No.	Species	Accession No.
1	*Pyrobaculum arsenaticum , strain PZ6*	AJ277124
2	*Pyrobaculum oguniense*	AB087402
3	*Sulfolobus tokodaii*	AB022438
4	*Stygiolobus azoricus*	D85520
5	*Thermoproteus tenax strain YS44*	AY538162
6	*Acidianus brierleyi strain DSM 1651*	NR_043409
7	*Acidianus ambivalens*	D85506
8	*Acidianus infernus*	D85505
9	Uncultured archaeon CRA8-27cm, marine sediment clone CRA8	AF119128
10	*Methanobacterium formicicum strain KOR-1*	JQ973735
11	*Methanobacterium formicicum strain MF*	NR_115168
12	*Methanobacterium formicicum strain DSM 1535*	NR_025028
13	*Methanosphaera stadtmanii*	M59139
14	*Methanosphaera stadtmanae DSM 3091*	AY196684
15	*Methanosphaera stadtmanae strain MCB-3*	NR_028236
16	*Methanobacterium thermoautotrophicum*	AB020530
17	*Methanothermobacter thermautotrophicus strain delta H*	NR_042782
18	*Methanothermobacter thermautotrophicus strain AM1*	HM228400
19	Uncultured Methanobacteriales archaeon clone OTU_970	KP902328
20	Uncultured Methanobacteriales archaeon from fresh water	LN796353
21	Uncultured Methanobacteriales archaeon, environmental samples	LN796417
22	*Methanobrevibacter arboriphilus strain DH-1*	AY196665
23	*Methanobrevibacter sp. ATM*	AF242652
24	*Methanobacterium ferruginis*	AB542743
25	*Methanobacterium petrolearium*	AB542742
26	*Methanobacterium bryantii strain MOH*	AY196657
27	*Methanobacterium oryzae*	AF028690
28	*Methanothermobacter wolfeii*	AB104858
29	*Halorubrum coriense*	L00922
30	*Halococcus dombrowskii*	AJ420376
31	*Haloarcula argentinensis*	D50849
32	*Halorubrum sodomense*	D13379
33	*Haloferax denitrificans*	D14128
34	*Haloferax alexandrinus*	AB037474
35	*Halogeometricum borinquense*	AF002984
36	Unidentified archaeon, clone pSSMCA108, from hydrothermal vent	AB019740
37	Unidentified archaeon, clone pMC2A10, from hydrothermal vent	AB019739
38	Uncultured archaeon 2MT1, from a Coastal Saltmarsh	AF015981
39	Uncultured archaeon CRA12-27cm	AF119123
40	Unidentified archaeon DNA, clone pMC2A203	AB019737
41	Uncultured archaeon TA1f2, from marine sediments	AF134390
42	Uncultured archaeon TA1c9	AF134388

43	Uncultured archaeon TA1e6, from marine sediments	AF134389
44	Uncultured archaeon 2C84, from Coastal Saltmarsh	AF015978
45	*Methanocalculus halotolerans,*	AF033672
46	*Methanoculleus bourgensis MS2*	AY196674
47	*Methanofollis sp. N2F9704*	AF262035
48	*Methanofollis tationis*	AF095272
49	*Methanofollis formosanus*	AY186542
50	*Methanospirillum lacunae*	AB517986
51	*Methanoculleus chikugoensis*	AB038795
52	Black sea cold seep, clone BS-K-F9	AJ578126
53	Santa Barbara Basin clone SB-24a1F10	AF354134
54	Santa Barbara Basin clone SB-24a1B11	AF354130
55	Hydrate Ridge, clone HydBeg134	AJ578116
56	Uncultured archaeon 2MT7 , a Coastal Saltmarsh	AF015991
57	Uncultured archaeon 2C83, a Coastal Saltmarsh	AF015977
58	Uncultured archaeon BA2H11fin, marine sediment	AF134393
59	Eel River Basin and Santa Barbara basin clone Eel-36a2A4	AF354128
60	Eel River Basin and Santa Barbara basin clone SB-24a1H2	AF354135
61	Eel River Basin and Santa Barbara basin clone SB-24a1C12	AF354138
62	Eel River Basin and Santa Barbara basin clone Eel-36a2B9	AF354140
63	Uncultured Methanosarcinales archaeon clone MOS1A_4113_G08	AY323222
64	Eel River Basin clone Eel-36a2A5	AF354133
65	Gulf of Mexico , Uncultured archaeon At425_ArD2	AY053472
66	Hydrate Ridge sediment clone Hyd24-Arch07a	AJ578112
67	Santa Barbara Basin clone SB-24a1A12	AF354131
68	Hydrate Ridge sediment clone Hyd24-Arch19	AJ578104
69	Santa Barbara Basin clone SB-17a1D3	AF354142
70	Santa Barbara Basin clone SB-17a1B11	AF354141
71	Hydrate Ridge Sediment clone HydBeg40	AJ578083
72	Eel River Basin clone Eel-36a2A1	AF354129
73	Gulf of Mexico, Uncultured archaeon AT425_ArE12	AY053474
74	Hydaret Ridge Sediment clone HydBeg125	AJ578115
75	Monterey Canyon, Calif. cold seep clone AMOS4A_4113_H05	AY323223
76	Guaymas Basin sediment clone C1_R019	AF 419638
77	Gulf of Mexico, clone GoM GC234 021R	AY211695
78	Gulf of Mexico gas hydrate clone GoM GC234 019R	AY211694
79	Hydrate Ridge sediment, clone HydBeg22	AJ578118
80	Hydrate Ridge sediment, clone HydBeg34	AJ578085
81	Hydrate Ridge sediment, clone HydCal75	AJ578092
82	Hydrate Ridge sediment , clone HydBeg149	AJ578117
83	Hydrate Ridge sediment, clone HydBeg41	AJ578095
84	Hydrate Ridge sediment, clone HydBeg05	AJ578098
85	Eel River Basin, Uncultured archaeon TA1a4	AF134384
86	Eel River Basin, Uncultured archaeon isolate Eel-36a2E1	AF354139
87	Guaymas Basin Sediment, clone C1_R048	AF419644

88	Gulf of Mexico, gas hydrate clone GoM GC234 634R	AY211713
89	Gulf of Mexico, gas hydrate clone GoM GC234 009R	AY211692
90	Monterey Canyon, Calif. Cold seep, clone AMOS1B_4113_F12	AY323221
91	Guaymas Basin sediment, clone AT_R007	AF419650
92	Hydrate Ridge sediment, clone fos0626f11	AJ890142
93	Hydrate Ridge sediment, clone fos0629b6	AJ890141
94	Mediterranean Sea mud volcano, clone AMSGC_32_A31	KF440345
95	Mediterranean Sea mud volcano	HQ588676
96	Eel River Basin, clone Eel-36a2H11	AF354136
97	Hydrate Ridge sediment, clone HydBeg92	AJ578119
98	Hydrate Ridge sediment, clone HMMVBeg-32	AJ579330
99	Haakon Mosby Mud Vulcano, clone HMMVBeg-34	AJ579327
100	*Methanococcus aeolicus Nankai-3*	DQ195164
101	*Methanothermococcus okinawensis*	AB057722
102	*Methanococcus vannielii*	AY196675
103	*Methanotorris formicicus*	AB100884
104	*Methanothermococcus thermolithotrophicus DSM 2095*	M59128
105	Black sea microbial mat, clone BS-S-D7	AJ578134
106	Black sea microbial mat, clone BS-SR-D3	AJ578141
107	Hydrate Ridge, clone HydCal52	AJ578120
108	Eel River Basin, clone Eel-36a2G10	AF354137
109	Black sea microbial mat, clone BS-S-H1	AJ578138
110	Hydrate Ridge, clone HydBeg01	AJ578084
111	Guaymas clone A1-R013	AF419625
112	Black sea microbial mat, clone BS-R-A1	AJ578131
113	Black sea microbial mat, clone BS-SR-C1-Arch	AJ578140
114	Black sea microbial mat, clone BS-M-A7	AJ578129
115	Black sea microbial mat, clone BSeua2	AF412943
116	Eel river, Uncultured archaeon BA2F4fin	AF134392
117	Eel river, Uncultured archaeon TA2e12	AF134391
118	Eel River, Uncultured archaeon BA1a1	AF134380
119	Eel River, Uncultured archaeon TA1a6	AF134386
120	Eel River, Uncultured archaeon BA1a2	AF134381
121	Eel River, Uncultured archaeon BA1b1	AF134382
122	Hydrothermal vent, clone pISA16	AB019758
123	Hydrothermal vent clone pISA14	AB019759

AppendixV. Gene organization in Dsr operon presented in contigs 00339 and 00237, and in three other *Desulfobacteraceae*. Green: Dissimilatory sulfite reductase alpha subunit (DsrA), Red: Dissimilatory sulfite reductase beta subunit (DsrB), Orange: Dissimilatory sulfite reductase clustered protein (DsrD), Blue: Cobyrinic acid A,C-diamide synthase. The latter is categorized in the Sulfite reduction-associated complex DsrMKJOP and co-clustering genes subsystem and its role is Cobyrinic acid A,C-diamide synthase.